Independent mechanisms of benzimidazole resistance across *Caenorhabditis* nematodes

Amanda O. Shaver[1]*, Ryan McKeown[2]*, Joyce M. Reyes Otero[1], and Erik C. Andersen[1]

[1] Dept. of Biology, Johns Hopkins University, Baltimore, Maryland, USA
[2] Dept. of Molecular Biosciences, Northwestern University, Evanston, Illinois, USA
* These authors contributed equally.

Corresponding author:
Erik C. Andersen
Johns Hopkins University
Department of Biology
3400 N. Charles St.
Bascom UTL 383
Baltimore, MD 21218
410-516-1282
erik.andersen@gmail.com

ORCIDs and emails:
Amanda O. Shaver: 0000-0002-2910-1505, amanda.shaver@jhu.edu, amandaoshaver@gmail.com
Ryan McKeown: 0000-0003-3570-2494, ryanmckeown2021@u.northwestern.edu
Joyce M. Reyes Otero: 0009-0002-5039-4434, joyce.reyes2@upr.edu
Erik C. Andersen: 0000-0003-0229-9651, erik.andersen@gmail.com

Keywords: Repeated evolution, *C. elegans*, *C. briggsae*, *C. tropicalis*, beta-tubulin, benzimidazoles

28 **ABBREVIATIONS**

ABZ	Albendazole
BZs	Benzimidazoles
Cbr-ben-1	*ben-1* in *Caenorhabditis briggsae*
Cbr-BEN-1	BEN-1 in *Caenorhabditis briggsae*
Cbr-tbb-1	*tbb-1* in *Caenorhabditis briggsae*
Cbr-TBB-1	TBB-1 in *Caenorhabditis briggsae*
Cbr-tbb-2	*tbb-2* in *Caenorhabditis briggsae*
Cbr-TBB-2	TBB-2 in *Caenorhabditis briggsae*
Cel-ben-1	*ben-1* in *Caenorhabditis elegans*
Cel-BEN-1	BEN-1 in *Caenorhabditis elegans*
Cel-tbb-1	*tbb-1* in *Caenorhabditis elegans*
Cel-TBB-1	TBB-1 in *Caenorhabditis elegans*
Cel-tbb-2	*tbb-2* in *Caenorhabditis elegans*
Cel-TBB-2	TBB-2 in *Caenorhabditis elegans*
Ctr-ben-1	*ben-1* in *Caenorhabditis tropicalis*
Ctr-BEN-1	BEN-1 in *Caenorhabditis tropicalis*
Ctr-tbb-1	*tbb-1* in *Caenorhabditis tropicalis*
Ctr-TBB-1	TBB-1 in *Caenorhabditis tropicalis*
Ctr-tbb-2	*tbb-2* in *Caenorhabditis tropicalis*
Ctr-TBB-2	TBB-2 in *Caenorhabditis tropicalis*
HSB	Horvitz Super Broth
HTA	High-throughput larval development assay
LoF	Loss-of-function
NGMA	Nematode growth media agar
SNV	Single nucleotide variants

54 SV Structural variants

55 **ABSTRACT**

56 Benzimidazoles (BZs), a widely used class of anthelmintic drugs, target beta-tubulin proteins,
57 disrupt microtubule formation, and cause nematode death. In parasitic nematode species,
58 mutations in beta-tubulin genes (*e.g.*, isotype-1 beta-tubulin) are predicted to inhibit BZ binding
59 and are associated with BZ resistance. Similarly, in the free-living nematode *Caenorhabditis*
60 *elegans*, mutations in an isotype-1 beta-tubulin ortholog, *ben-1*, are the primary drivers of BZ
61 resistance. The recurrent association of BZ resistance with beta-tubulins suggests that BZ
62 resistance is repeatedly caused by mutations in beta-tubulin genes, an example of repeated
63 evolution of drug resistance across nematode species. To evaluate the hypothesis of repeated
64 evolution of BZ resistance mediated by beta-tubulin, we identified predicted resistance alleles in
65 beta-tubulin genes across wild strains from three *Caenorhabditis* species: *C. elegans*,
66 *Caenorhabditis briggsae*, and *Caenorhabditis tropicalis*. We hypothesized that, if these species
67 experienced similar selective pressures, they would evolve resistance to BZs by mutations in any
68 of three beta-tubulin genes (*ben-1*, *tbb-1*, and *tbb-2*). Using high-throughput development assays,
69 we tested the association of predicted beta-tubulin alleles with BZ resistance. We found that a
70 heterogeneous set of variants identified in *C. elegans ben-1* were associated with BZ resistance.
71 In *C. briggsae*, only two variants in *ben-1*, predicted to encode a premature stop codon (W21stop)
72 and a missense substitution (Q134H), were associated with BZ resistance. In *C. tropicalis*, two
73 missense variants were identified in *ben-1*, but neither was associated with BZ resistance. *C.*
74 *briggsae* and *C. tropicalis* might have evolved BZ resistance by mutations in other beta-tubulin
75 genes, but we found that variants in *tbb-1* or *tbb-2* in these species were not associated with BZ
76 resistance. Our findings reveal a lack of repeated evolution of BZ resistance across the three
77 *Caenorhabditis* species and highlight the importance of defining BZ resistance mechanisms
78 outside of beta-tubulins.

1. INTRODUCTION

Global control of parasitic nematode infections relies on the efficacy of a small arsenal of anthelmintic drugs, including benzimidazoles (BZs) (A. C. Kotze et al. 2020). BZs are a widely used class of anthelmintic drugs that target beta-tubulin proteins (Lubega and Prichard 1990), disrupt microtubule formation (Neff et al. 1983; Laclette, Guerra, and Zetina 1980; Ireland et al. 1979), and lead to nematode death. Although BZs are essential in human and veterinary medicine, resistance is prominent in parasitic nematode populations (Theodorides, Scott, and Lademan 1970; Roos, Kwa, and Grant 1995). To effectively screen for and manage the emergence of BZ resistance, it is necessary to understand the underlying genetics that contribute to the evolution of BZ resistance in nematode species.

Historically, BZ resistance in parasite populations (*i.e.*, *Haemonchus contortus*, *Teladorsagia circumcincta*, and *Trichostrongylus colubriformis*) has been associated with three canonical missense variants (F167Y, E198A, and F200Y) in orthologs of the *H. contortus isotype-1* (Silvestre and Cabaret 2002; Ghisi, Kaminsky, and Mäser 2007; de Lourdes Mottier and Prichard 2008; Kwa, Veenstra, and Roos 1994) and *isotype-2 beta-tubulin* genes (A. C. Kotze and Prichard 2016; Avramenko et al. 2019). These three missense variants have been used to track and manage BZ resistance across nematode species globally (Kwa, Veenstra, and Roos 1994; Silvestre and Cabaret 2002; Ghisi, Kaminsky, and Mäser 2007). However, these three missense variants do not explain all of the BZ resistance observed in parasitic nematode populations (Andrew C. Kotze et al. 2014; Krücken et al. 2017). Recently, additional novel missense variants have been associated with BZ resistance (*e.g.*, E198I, E198K, E198T, E198stop, and Q134H) (Venkatesan et al. 2023; Mohammedsalih et al. 2020). The three canonical missense variants, along with novel missense variants of these parasitic nematode beta-tubulin alleles, conferred BZ resistance when introduced in the free-living nematode *Caenorhabditis elegans* (Dilks et al. 2020, 2021). Unlike parasitic species, *C. elegans* wild strains

104 have a heterogeneous set of variants in one of the *isotype-1 beta-tubulin* orthologs, *ben-1*,
105 responsible for much of BZ resistance in the species (Hahnel et al. 2018). The recurrent
106 association of BZ resistance with alleles predicted to impact beta-tubulin function across
107 nematode species suggests that BZ resistance repeatedly evolves by standing variation or
108 recurrent mutations in beta-tubulin genes and provides compelling evidence to predict the
109 emergence of BZ resistance across nematode species.

110 Repeated evolution is the development of a similar phenotype (*e.g.*, BZ resistance) and
111 genotype (*e.g.*, the same beta-tubulin alleles confer BZ resistance) in response to similar
112 environmental pressures (*e.g.*, BZ exposure) (Cerca 2023). Because parasitic and free-living
113 nematodes have evolved BZ resistance by variants in conserved beta-tubulin genes, we
114 hypothesized that nematodes acquire BZ resistance by repeated variants or mutations in beta-
115 tubulin genes. However, this hypothesis is difficult to test directly in parasitic nematode species
116 because of their host-dependent life cycles, poorly annotated reference genomes, and limited
117 molecular and genetic tools (Hahnel et al. 2020; Mariene and Wasmuth 2025). By contrast, the
118 availability of high-quality genomic data for hundreds of wild strains (Crombie et al. 2023) and the
119 laboratory tractability of the free-living *Caenorhabditis* nematode species (*C. elegans*,
120 *Caenorhabditis briggsae*, and *Caenorhabditis tropicalis*) provide an opportunity to test for the
121 repeated evolution of BZ resistance in the *Caenorhabditis* genus.

122 Using the global natural diversity of *C. elegans*, *C. briggsae*, and *C. tropicalis*, we
123 assessed variation in conserved beta-tubulin genes to identify predicted BZ resistance alleles.
124 We identified single nucleotide variants (SNVs), small insertions or deletions (INDELs), and
125 structural variants (SVs) predicted to impact function in conserved beta-tubulin genes, herein
126 called “high-impact” variants. Because high-impact variants in the *Cel-ben-1* gene are known to
127 account for much of the BZ resistance in *C. elegans*, we first used an established high-throughput
128 larval development assay (HTA) to expose *C. elegans* strains with novel *ben-1* variants to the
129 prominently used BZ, albendazole (ABZ), to identify new resistance alleles. We found eight novel

130 variants in *Cel-ben-1*, of which six were associated with ABZ resistance in the HTAs, a result that
131 further confirms the role *Cel-ben-1* plays in ABZ resistance. Next, we used the HTA to expose
132 *C. briggsae* and *C. tropicalis* strains with novel *ben-1* variants to ABZ to identify if these two
133 species confer ABZ resistance by the same mechanism as in *C. elegans*. In *C. briggsae*, two of
134 the eleven BEN-1 variants (W21stop and Q134H) were correlated with ABZ resistance. In *C.*
135 *tropicalis*, neither of the two BEN-1 variants (P80T and R121Q) were associated with ABZ
136 resistance. Because we found a lack of repeated evolution of BZ resistance by variants in *ben-1*,
137 we tested whether *C. briggsae* and *C. tropicalis* evolved BZ resistance by variants in the beta-
138 tubulin genes *tbb-1* and *tbb-2*, but found no high-impact variants in these genes associated with
139 ABZ resistance. Overall, our results indicate a lack of repeated evolution of ABZ resistance across
140 *Caenorhabditis* species, suggesting that beta-tubulin cannot underlie BZ resistance across all
141 nematode species.

142 2. MATERIALS AND METHODS

143 2.1 Identification of beta-tubulin loci

144 Amino acid sequences for all six *C. elegans* beta-tubulin proteins were obtained from
145 WormBase (WS283) (Sternberg et al. 2024) and used as queries in a BLASTp search (Version
146 2.12.0) (Camacho et al. 2009). The search was performed against protein sequence databases
147 constructed using gene models for *C. briggsae* (Moya et al. 2023) and *C. tropicalis* (Noble et al.
148 2021). To construct the protein sequence database, we extracted gene model transcript features
149 from the gene feature file with *gffread* (Version 0.9.11) (Pertea and Pertea 2020) and processed
150 them using the *makeblastdb* function from BLAST (Version 2.12.0). From the BLASTp search, we
151 identified *C. briggsae* and *C. tropicalis* protein sequences with the highest percent identity (PID)
152 to each *C. elegans* beta-tubulin protein. Only protein sequences with the highest PID in both
153 searches were considered orthologs (**S1 Table**). For some *C. elegans* beta-tubulin orthologs,

154 multiple *C. briggsae* or *C. tropicalis* gene models contained multiple splice isoforms. All gene
155 models for all beta-tubulin transcripts were manually inspected, and isoforms that were not fully
156 supported by short-read RNA sequencing data were removed.
157
158 **2.2 Single nucleotide variant (SNV) and indel calling and annotation**
159 To identify single nucleotide variants (SNVs) or indels (insertions and deletions) in the
160 beta-tubulin genes across the selfing *Caenorhabditis* species, we used the Variant Annotation
161 Tool from the *Caenorhabditis* Natural Diversity Resource (CaeNDR) (Release IDs: *C. elegans* -
162 20231213, *C. briggsae* - 20240129, *C. tropicalis* - 20231201) (Crombie et al. 2023). The identified
163 SNVs and indels (**S2, S3, and S4 Tables**) included small insertions and deletions, frameshifts,
164 altered stop and start codons, nonsynonymous changes, and splice variants.
165
166 **2.3 Structural variant (SV) calling and annotation**
167 Structural variant (SV) calling was performed using *DELLY* (Version 0.8.3), a SV caller
168 optimized to detect large insertions, deletions, and other complex structural variants such as
169 inversions, translocations, and duplications in paired-end short-read alignments (Rausch et al.
170 2012) and shown to perform well on *C. elegans* short-read sequence data (Lesack et al. 2022).
171 SVs that overlapped with beta-tubulin genes were extracted using *bcftools* (Version 1.10.1)
172 (Danecek et al. 2021). Insertions, deletions, inversions, and duplications that passed the *DELLY*
173 (Version 0.8.3) default quality threshold (greater than three supporting read pairs with a median
174 MAPQ > 20), filtered to high-quality genotypes (genotype quality > 15), and had at least one
175 alternative allele were retained. For complex variants (inversions and duplications), the
176 identification of at least one split-read pair was required (variants flagged as a precise SV by
177 *DELLY*). To validate SVs that passed quality filtering, each SV was manually inspected for
178 breakpoints in the raw-read alignments (*Wally*, Version 0.5.8) and for impacts on the beta-tubulin
179 coding sequence (CaeNDR Genome Browser) (Crombie et al. 2023) (**S5 Table**). We retained

180 SVs where raw read alignments suggested that the SV impacted the beta-tubulin coding
181 sequence. We compared the *Cel-ben-1* SVs called by *DELLY* to those SVs identified previously
182 (Hahnel et al. 2018). *DELLY* successfully recalled structural variants in several strains, including
183 deletions in JU751, JU830, JU1395, JU2582, JU2587, JU2593, JU2829, and QX1233, as well as
184 an inversion in MY518. However, *DELLY* did not detect a previously reported transposon insertion
185 in strain JU3125. To assess if other SVs could have been missed by *DELLY*, we manually
186 inspected the read alignments for all strains that had not been previously phenotyped to check if
187 any other SVs were not detected by *DELLY*. We confirmed the presence of novel *Cel-ben-1* SVs
188 in multiple strains, including deletions in ECA706 and NIC1832, and a duplication in NIC1107.
189 Additionally we identified a previously undetected deletion in JU4287.
190

191 **2.4 Association of low *Cel-ben-1* expression with ABZ response**

192 Two previous assays measured developmental responses of wild *C. elegans* strains after
193 ABZ exposure (Hahnel et al. 2018; Shaver et al. 2023). For 180 of these wild *C. elegans* strains,
194 expression levels (transcripts per million estimates [TPM]) were collected at the young-adult stage
195 (Zhang et al. 2022). Of the 180 wild *C. elegans* strains, 105 strains were shared between both
196 assays. A linear model was built using the *lm* function in R to account for assay effects.
197 Subsequently, the residuals of the linear model were used to normalize previous measures of
198 ABZ response. We evaluated the linear fit between each strain's expression of *ben-1*, *tbb-1*, or
199 *tbb-2* and the developmental delay following ABZ exposure.
200

201 **2.5 Phylogenetic analysis**

202 We characterized the relatedness of isotype reference strains (genetically unique strains)
203 with beta-tubulin variants using species trees downloaded from CaeNDR and generated by the
204 'post-gatk-nf' pipeline (https://github.com/AndersenLab/post-gatk-nf) (Release IDs: *C. elegans* -
205 20231213, *C. briggsae* - 20240129, *C. tropicalis* - 20231201) (Crombie et al. 2023). Briefly, the

206 trees were generated with high-quality SNVs in isotype reference strains retained in the hard-
207 filtered variant call format (VCF) file. *vcf2phylip* (Ortiz 2019) and the *bioconvert* (Caro et al. 2023)
208 function *phylip2stockholm* were used to prepare inputs for *quicktree*, which was used to construct
209 a tree using a neighbor-joining algorithm (Saitou and Nei 1987). All versions of these software
210 can be accessed from the 'post-gatk' docker container
211 (https://hub.docker.com/r/andersenlab/tree), used by the 'post-gatk-nf' pipeline. We visualized the
212 trees for each species using the *ggtree* function from the *ggtree* (v3.6.2) R package (Yu 2020).
213
214 **2.6 Strain selection and maintenance**
215 Fifteen *C. elegans* strains, 38 *C. briggsae* strains, and seven *C. tropicalis* strains from the
216 CaeNDR (Crombie et al. 2023) were used in this study (**S2, S3, and S4 Tables)**. Isolation details
217 for each strain are included in CaeNDR. For each species, we selected strains that had unique
218 high-impact consequences (SNV or SV) in *ben-1*, *tbb-1*, or *tbb-2* that had not been previously
219 phenotyped. Strains with high-impact consequences in a beta-tubulin gene are herein referred to
220 as "predicted resistant" strains. Strains with no high-impact consequences in beta-tubulin genes
221 that were closely related to predicted resistant strains were also included for *C. briggsae* and *C.*
222 *tropicalis* and herein classified as "predicted susceptible" strains (**S3 and S4 Figures**) (**Table S6**).
223 The reference strain(s) for all three species was included. Finally, for *C. elegans*, a strain with a
224 loss of *ben-1* (ECA882) was also included.
225 Before measuring ABZ responses, *C. elegans* and *C. briggsae* animals were maintained
226 at 20ºC and *C. tropicalis* animals were maintained at 25ºC. All animals were maintained on 6 cm
227 plates with modified nematode growth medium (NGMA), which contains 1% agar and 0.7%
228 agarose to prevent animals from burrowing (Andersen et al. 2014). The NGMA plates were
229 seeded with the *Escherichia coli* strain OP50 as a nematode food source. All strains were grown
230 for three generations without starvation on NGMA plates before anthelmintic exposure to reduce
231 the transgenerational effects of starvation stress (Andersen et al. 2015).

232

233 **2.7 Nematode food preparation for NGMA 6 cm plates**

234 A batch of OP50 *E. coli* was grown and used as a nematode food source for NGMA plates.
235 A frozen stock of OP50 *E. coli* was streaked onto a 10 cm Luria-Bertani (LB) agar plate and
236 incubated overnight at 37ºC. The following day, a single bacterial colony was transferred into two
237 culture tubes that contained 5 mL of 1x LB. The starter cultures and two negative controls (1X LB
238 without *E. coli*) were incubated for 18 hours at 37ºC shaking at 210 rpm. The OD_{600} value of the
239 starter cultures were measured using a spectrophotometer (BioRad, SmartSpec Plus) to calculate
240 how much starter culture was needed to inoculate a 1 L culture at an OD_{600} value of 0.005. For
241 each assay, one culture containing one liter of pre-warmed 1X LB inoculated with the starter
242 culture grew for approximately 4 - 4.5 hours at 37ºC at 210 rpm to an OD_{600} value between 0.45
243 and 0.6. Cultures were transferred to 4ºC to slow growth. OP50 was spotted on NGMA test plates
244 (two per culture) and grown at 37ºC overnight to ensure no contamination.

245

246 **2.8 Nematode food preparation for HTAs**

247 One batch of HB101 *E. coli* was used as a nematode food source for all HTAs in this
248 study. A frozen stock of HB101 *E. coli* was streaked onto a 10 cm LB agar plate and incubated
249 overnight at 37ºC. The following day, a single bacterial colony was transferred into three culture
250 tubes that contained 5 mL of 1x Horvitz Super Broth (HSB). The starter cultures and two negative
251 controls (1X HSB without *E. coli*) were incubated for 18 hours at 37ºC shaking at 180 rpm. The
252 OD_{600} value of the starter cultures were measured using a spectrophotometer (BioRad,
253 SmartSpec Plus) to calculate how much starter culture was needed to inoculate a 1 L culture at
254 an OD_{600} value of 0.001. A total of four cultures each containing 1 L of pre-warmed 1X HSB
255 inoculated with the starter culture grew for 15 hours at 37ºC while shaking at 180 rpm. After 15
256 hours, flasks were removed from the incubator and transferred to 4ºC to slow growth. The 1X
257 HSB was removed from the cultures by performing three rounds of centrifugation, where the

258 supernatant was removed, and the bacterial cells were pelleted. Bacterial cells were washed with
259 K medium, resuspended in K medium, pooled, and transferred to a 2 L glass beaker. The OD_{600}
260 value of the bacterial suspension was measured and diluted to a final concentration of OD_{600}100
261 with K medium, aliquoted to 15 mL conicals, and stored at -80ºC for use in the HTAs.
262

263 **2.9 ABZ dose-response assays for *C. briggsae* and *C. tropicalis***

264 Because ABZ response has been minimally characterized in *C. briggsae* (Zamanian et al.
265 2018) and has not yet been described in *C. tropicalis*, we first measured dose-response curves
266 for both species after exposure to ABZ to assess developmental delay. Before performing HTAs,
267 ABZ (Sigma-Aldrich, Catalog # A4673-10G) stock solutions were prepared in dimethyl sulfoxide
268 (DMSO) (Fisher Scientific, Catalog # D1281), aliquoted, and stored at -20ºC for use in the assays.
269 For the dose-response assays, animals were exposed to ABZ at the following concentrations
270 (µM): 0 (1% DMSO), 0.12, 0.23, 0.47, 0.94, 1.88, 3.75, 7.5, 15, 30, 60, and 120. Animals were
271 allowed to develop in the presence of ABZ as described in *HTAs to assess nematode*
272 *development*.

273 Dose-response model estimation and statistics were performed as described previously
274 (Widmayer et al. 2022; Shaver et al. 2023). Briefly, a four-parameter log-logistic dose-response
275 curve was fit independently for a genetically diverse set of 11 *C. briggsae* strains (**S5 Figure**) and
276 seven *C. tropicalis* strains (**S6 Figure**), where normalized median animal length was used as a
277 metric for phenotypic response (see *Methods*). For each strain-specific dose-response model,
278 slope (b) and concentration (e) were estimated with strain as a covariate. We calculated EC_{10} as
279 we have previously found EC_{10} response to be more heritable than half maximal effective
280 concentration (EC_{50}) estimates and were therefore used in our analysis (Shaver et al. 2023;
281 Widmayer et al. 2022). A dosage of 30 µM ABZ was closest to the EC_{10} for *C. briggsae* and *C.*
282 *tropicalis*, consistent with ABZ concentrations used in past *C. elegans* assays (Dilks et al. 2020,
283 2021; Shaver et al. 2024) and in all HTAs in this study.

284

285 **2.10 HTAs to assess nematode development**

286 Populations of each strain were amplified and bleach-synchronized in three independent
287 assays. Independent bleach synchronizations controlled for variation in embryo survival and
288 subsequent effects on developmental rates. After bleach synchronization, approximately 30
289 embryos were dispensed into the wells of a 96-well microplate in 50 µL of K medium. Forty-eight
290 wells were prepared per bleach for each strain. Each 96-well microplate was prepared, labeled,
291 and sealed using gas-permeable sealing films (Fisher Scientific, Catalog # 14-222-043). Plates
292 were placed in humidity chambers to incubate for 24 hours at 20°C while shaking at 170 rpm
293 (INFORS HT Multitron shaker). After 24 hours, every plate was inspected to ensure that all
294 embryos hatched and animals were developmentally arrested at the first larval (L1) stage so all
295 strains started each assay at the same developmental stage. Next, food was prepared to feed the
296 developmentally arrested L1 animals using the required number of OD_{600}100 HB101 aliquots (see
297 *Nematode food preparation for HTAs*). The HB101 aliquots were thawed at room temperature,
298 combined into a single conical tube, and diluted to an OD_{600}30 with K medium. To inhibit further
299 bacterial growth and prevent contamination, 150 µL of kanamycin was added to the HB101. An
300 aliquot of 100 µM ABZ stock solution was thawed at room temperature and added to an aliquot
301 of OD_{600}30 K medium at a 3% volume/volume ratio. Next, 25 µL of the food and ABZ mixture was
302 transferred into the appropriate wells of the 96-well microplates to feed the arrested L1 animals
303 at a final HB101 concentration of OD_{600}10 and expose L1 animals to ABZ. Immediately afterward,
304 the 96-well microplates were sealed using a new gas permeable sealing film, returned to the
305 humidity chambers, and incubated for 48 hours at 20°C (*C. elegans* and *C. briggsae*) or 25°C (*C.*
306 *tropicalis*) while shaking at 170 rpm. After 48 hours (*C. elegans* and *C. briggsae*) or 42 hours (*C.*
307 *tropicalis*) of incubation and shaking in the presence of food and either DMSO or ABZ, the 96-
308 well microplates were removed from the incubator and treated with 50 mM sodium azide in M9
309 for 10 minutes to paralyze and straighten nematodes. After 10 minutes, images of nematodes in

310 the microplates were immediately captured using Molecular Devices ImageXpress Nano
311 microscope (Molecular Devices, San Jose, CA) using a 2X objective. The ImageXpress Nano
312 microscope acquires brightfield images using a 4.7 megapixel CMOS camera and stores images
313 in a 16-bit TIFF format. The images were used to quantify the development of nematodes in the
314 presence of DMSO or ABZ as described below (see *High-throughputput imager assays [HTA]*
315 *data collection and cleaning*). A full step-by-step protocol for the HTA has been deposited in
316 protocols.io.
317
318 **2.11 HTA data collection and data cleaning**
319 *CellProfiler* (Version 24.10.1) was used to characterize and quantify biological data from
320 the image-based assays. Custom software packages designed to extract animal measurements
321 from images collected on the Molecular Devices ImageXpress Nano microscope were previously
322 described (Nyaanga et al. 2021). *CellProfiler* modules and *Worm Toolbox* were developed to
323 extract morphological features of individual animals from images from the HTA (Wählby et al.
324 2012). Worm model estimations and custom *CellProfiler* pipelines were written using the
325 *WormToolbox* in the GUI-based instance of *CellProfiler* (Widmayer et al. 2022). Next, a Nextflow
326 pipeline (Version 24) was written to run command-line instances of *CellProfiler* in parallel on the
327 Rockfish High-Performance Computing Cluster (Johns Hopkins University). The *CellProfiler*
328 workflow can be found at https://github.com/AndersenLab/cellprofiler-nf. The custom *CellProfiler*
329 pipeline generates animal measurements by using four worm models: three worm models tailored
330 to capture animals at the L4 larval stage, in the L2 and L3 larval stages, and the L1 larval stage,
331 as well as a “multi-drug high dose” (MDHD) model, to capture animals with more abnormal body
332 sizes caused by extreme anthelmintic responses. These measurements comprised our raw
333 dataset. Two *C. briggsae* strains (NIC1052 and VX34) were not fully paralyzed and straightened
334 at the time of imaging, which created some misclassification of animal measurements. Thus, the
335 animal lengths for strains NIC1052 and VX34 measured by CellProfiler are shorter than the actual

336 animal lengths. However, the difference discrepancy in animal lengths does not affect the
337 classification of a strain as resistant or sensitive to ABZ. Data cleaning and analysis steps were
338 performed using a custom R package, *easyXpress* (Version 2.0) (Nyaanga et al. 2021) and
339 followed methods previously reported (Shaver et al. 2024). All analyses were performed using
340 the R statistical environment (Version 4.2.1) unless stated otherwise.
341

342 **3. RESULTS**

343 **3.1 In three free-living *Caenorhabditis* species, strains with high-impact variants in beta-**
344 **tubulin genes or low levels of beta-tubulin expression are predicted to confer ABZ**
345 **resistance**

346 To investigate if the mechanisms of ABZ resistance are repeated across the three selfing
347 *Caenorhabditis* species, we identified "predicted resistant" strains that have high-impact variants
348 (*i.e.*, SNVs, INDELs, or SVs) (Crombie et al. 2023) likely to affect the function of the five conserved
349 beta-tubulin genes (*i.e.*, *ben-1*, *tbb-1*, *tbb-2*, *tbb-4*, and *mec-7*) (see *Methods*). Although ABZ
350 response has been highly characterized and associated with mutations in *ben-1* across *C.*
351 *elegans* wild strains (Hahnel et al. 2018; Shaver et al. 2024), less is known about how *C. briggsae*
352 (Zamanian et al. 2018) and *C. tropicalis* respond to ABZ exposure. To minimize the amount of
353 genetic variation outside of the beta-tubulin that could affect the BZ response, we also selected
354 *C. briggsae* and *C. tropicalis* strains that lacked high-impact variants in beta-tubulin genes but
355 were closely related to predicted resistant strains (**S3 and S4 Figures**). The strains with no high-
356 impact variants in any beta-tubulin gene were classified as "predicted susceptible".

357 In a set of 611 *C. elegans* strains (Crombie et al. 2023), we identified 65 strains with 33
358 unique high-impact variants in *Cel-ben-1* (**Table S2**). Of the 33 unique high-impact variants, 24
359 were previously phenotyped and 23 were associated with ABZ resistance (**S1A Figure**) (Hahnel
360 et al. 2018; Shaver et al. 2024). Here, we report eight novel high-impact variants predicted to
361 impact *Cel*-BEN-1 (E3stop, Y50C, P80S, VDN113N, frameshift 319, frameshift 368, stop445S,

362 and a duplication) that have not previously associated with ABZ resistance in nematodes (**Table**
363 **S2**). The missense variants predicted to encode Y50C and P80S *Cel*-BEN-1 substitutions have
364 been found in fungus and human beta-tubulins, respectively (Qiu et al. 2011; Dingerdissen et al.
365 2018). We found no strains with high-impact variants predicted to impact *Cel*-TBB-1 or *Cel*-TBB-
366 2.

367 Previously, low *ben-1* expression was correlated with ABZ resistance in *C. elegans* strains
368 (Zhang et al. 2022), providing another parameter to investigate BZ resistance across the species.
369 We evaluated if beta-tubulin expression levels were predictive of ABZ responses in *C. elegans.*
370 We used a linear regression model to assess the relationship between the expression of *Cel-ben-*
371 *1*, *Cel-tbb-1*, or *Cel-tbb-2* (Zhang et al. 2022) and ABZ responses in 180 wild strains (Hahnel et
372 al. 2018; Shaver et al. 2024). We found a significant negative relationship between *Cel-ben-1*
373 expression (>=3.75 TPM) and ABZ resistance (p-value = 5.16e-16, r^2= 0.344) (**S1 Figure**).
374 Importantly, 19 of the 23 strains with low *ben-1* expression also had high-impact variants in *ben-*
375 *1* (SVs, frameshifts, or stop/start altering variants). Next, we identified strains with no high-impact
376 variants in *ben-1* but had low *ben-1* expression that we predicted to cause ABZ resistance. Using
377 these parameters, we found one strain, JU1581, with low *Cel-ben-1* expression to test for ABZ
378 resistance and to further define the role *Cel-ben-1* plays in ABZ resistance. No significant
379 relationship was found between *Cel-tbb-2* and *Cel-tbb-1* expression and ABZ response (**S2**
380 **Figure**).

381 In a set of 641 *C. briggsae* strains, we identified 22 strains with eight unique high-impact
382 variants in *Cbr-ben-1* (**Table S3**). The eight unique high-impact variants in *Cbr*-BEN-1 included
383 seven amino acid substitutions (V91I, Q94K, D128E, Q134H, S218L, M299V, and R359H) and
384 one premature stop codon (W21stop). Outside of *Cbr*-BEN-1, we identified missense variants in
385 *Cbr*-TBB-1 (T35A, A275T, L377I, and V64I) and *Cbr*-TBB-2 (E441A) predicted to disrupt function.
386 All *C. briggsae* predicted resistant strains, predicted susceptible strains, and the reference strains
387 (AF16 and QX1410) (Stevens et al. 2022; Moya et al. 2023) were phenotyped for ABZ response

388 (**S1 Figure**).

389 In a set of 518 *C. tropicalis* strains, we identified two strains with unique high-impact
390 variants in *Ctr*-BEN-1 (**Table S4**) (P80T and R121Q). Outside of *Ctr*-BEN-1, we identified one
391 missense variant in *Ctr*-TBB-2 (N89S) and no high-impact variants in *Ctr*-TBB-1. All *C. tropicalis*
392 predicted resistant strains, three predicted susceptible strains, and the reference strain (NIC58)
393 (Luke et al. 2021) were phenotyped for ABZ response.

394

395 **3.2 Natural allelic variation in *ben-1* is associated with ABZ resistance in *C. elegans***

396 We performed image-based HTAs across all *C. elegans* wild strains with novel high-
397 impact variants in *ben-1* (*i.e.*, predicted resistant strains) to measure nematode length (a proxy
398 for larval development) in drug (ABZ) and control (DMSO) conditions (see *Methods*). The
399 canonical laboratory strain N2 was included as an ABZ-susceptible control (Dilks et al. 2020,
400 2021; Shaver et al. 2024) and a strain with the loss of *ben-1* in the N2 strain background (ECA882)
401 was included as an ABZ-resistant control. Previously, two high-impact variants (frameshift at
402 position 299 and a deletion) were associated with ABZ resistance (Hahnel et al. 2018; Dilks et al.
403 2020). With expanded sampling, we identified two novel strains with the same frameshift at
404 position 299 (JR4305) and the same deletion (NIC1832) in *Cel-ben-1*. Therefore, we included
405 JR4305 and NIC1832 to validate the role that a frameshift at position 299 and a deletion play in
406 ABZ resistance. The assay included 48 replicates per strain with 5 to 30 animals per replicate in
407 ABZ or DMSO conditions. The reported nematode length of each strain is the delta between
408 animal lengths in DMSO (**S7 Figure**) and ABZ to obtain normalized animal length and assess
409 drug effects. We classified a strain as resistant to ABZ if its nematode length after ABZ exposure
410 was 75% greater than that of the reference strain (see *Methods*). A longer median animal length
411 (*i.e.*, larger animals) indicated resistance to ABZ, and a shorter median animal length (*i.e.*, smaller
412 animals) indicated susceptibility to ABZ.

413 As expected, when exposed to ABZ, strains ECA882 (loss of *ben-1*), JR4305 (frameshift

414 at position 299), and NIC1832 (deletion) all recapitulated a resistance phenotype (nematode
415 length ≥ 75% of the reference strain N2). Of the eight predicted resistant *C.elegans* strains, six
416 displayed a resistance phenotype (**Fig. 1**). All six wild strains showed minimal developmental
417 delays after exposure to ABZ, a phenotype similar to loss of *ben-1* (**Fig. 1**). Of all the assayed
418 predicted resistant strains with variants in *Cel*-BEN-1, three (P80S, stop445S, and low *ben-1*
419 expression) were not classified as resistant to ABZ. The P80S variant might partially alter *ben-1*
420 function, causing a moderate resistance phenotype. In stop445S, the normal stop codon was
421 replaced with a serine, likely allowing translation to continue beyond the termination point. This
422 variant likely does not affect *ben-1* function because position 445 is at the end of the BEN-1
423 protein. Finally, the strain with low *ben-1* expression (JU1581), which did not have any high-
424 impact variants in *ben-1*, was sensitive to ABZ, indicating that the selected threshold of *ben-1*
425 expression (≥3.75 TPM) still retained strains with adequate *ben-1* function.

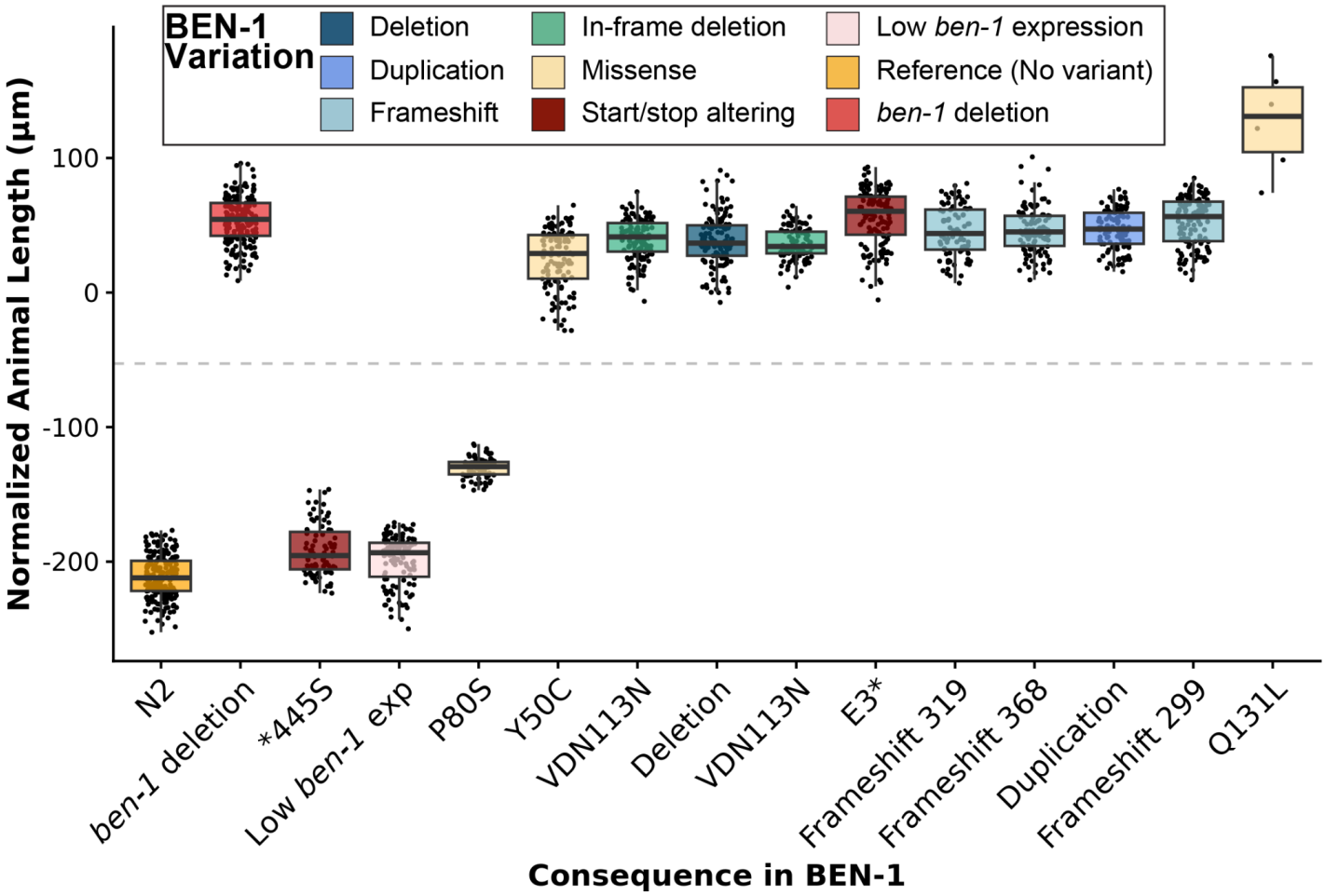

Figure 1. High-throughput assays for each *C. elegans* strain with a high-impact variant in BEN-1 in the presence of albendazole

The regressed median animal length values for populations of nematodes grown in 30 µM albendazole (ABZ) are shown on the y-axis. Each point represents the normalized median animal length value of a well containing approximately 5-30 animals. Strains are sorted by their relative resistance to ABZ based on median animal length. Data are shown as Tukey box plots with the median as a solid horizontal line, and the top and bottom of the box representing the 75th and 25th quartiles, respectively. The top whisker is extended to the maximum point that is within the 1.5 interquartile range from the 75th quartile. The bottom whisker is extended to the minimum point that is within the 1.5 interquartile range from the 25th quartile. Strains are colored by beta-tubulin variant status. The gray dashed line marks the resistance threshold (nematode length ≥ 75% of the reference strain N2).

3.3 Rare missense and nonsense variants in *Cbr-ben-1* are associated with ABZ resistance,

440 **whereas high-impact variants in *Ctr-ben-1* are not**

441 We performed HTAs on 11 predicted resistant *C. briggsae* strains with eight unique
442 variants in *Cbr-ben-1* and on 13 predicted susceptible strains in DMSO (**S8 Figure**) and ABZ
443 conditions. We found that in *C. briggsae*, only two variants in BEN-1 (Q134H and W21stop)
444 conferred ABZ resistance (nematode length ≥ 75% of the reference strain AF16) (**Fig. 2**). The
445 Q134H amino acid change has been associated with ABZ resistance in *Ancylostoma caninum*
446 and validated in *C. elegans* (Venkatesan et al. 2023). An early stop gain at position 21 is predicted
447 to cause the premature termination of protein synthesis and *Cbr-ben-1* loss-of-function (LoF). Of
448 all the assayed strains with predicted resistance variants in *Cbr*-BEN-1, six (V91I, Q94K, D128E,
449 S218L, M299V, and R359H) were not resistant to ABZ. Overall, because only one of the seven
450 missense variants was associated with ABZ resistance, we could not reliably predict how a strain
451 responded to ABZ based on the presence of a missense variant alone. These results indicate that
452 ABZ resistance associated with *Cbr-ben-1* variants is uncommon and that accurately predicting
453 ABZ resistance in *C. briggsae* requires additional factors beyond *ben-1* variation.

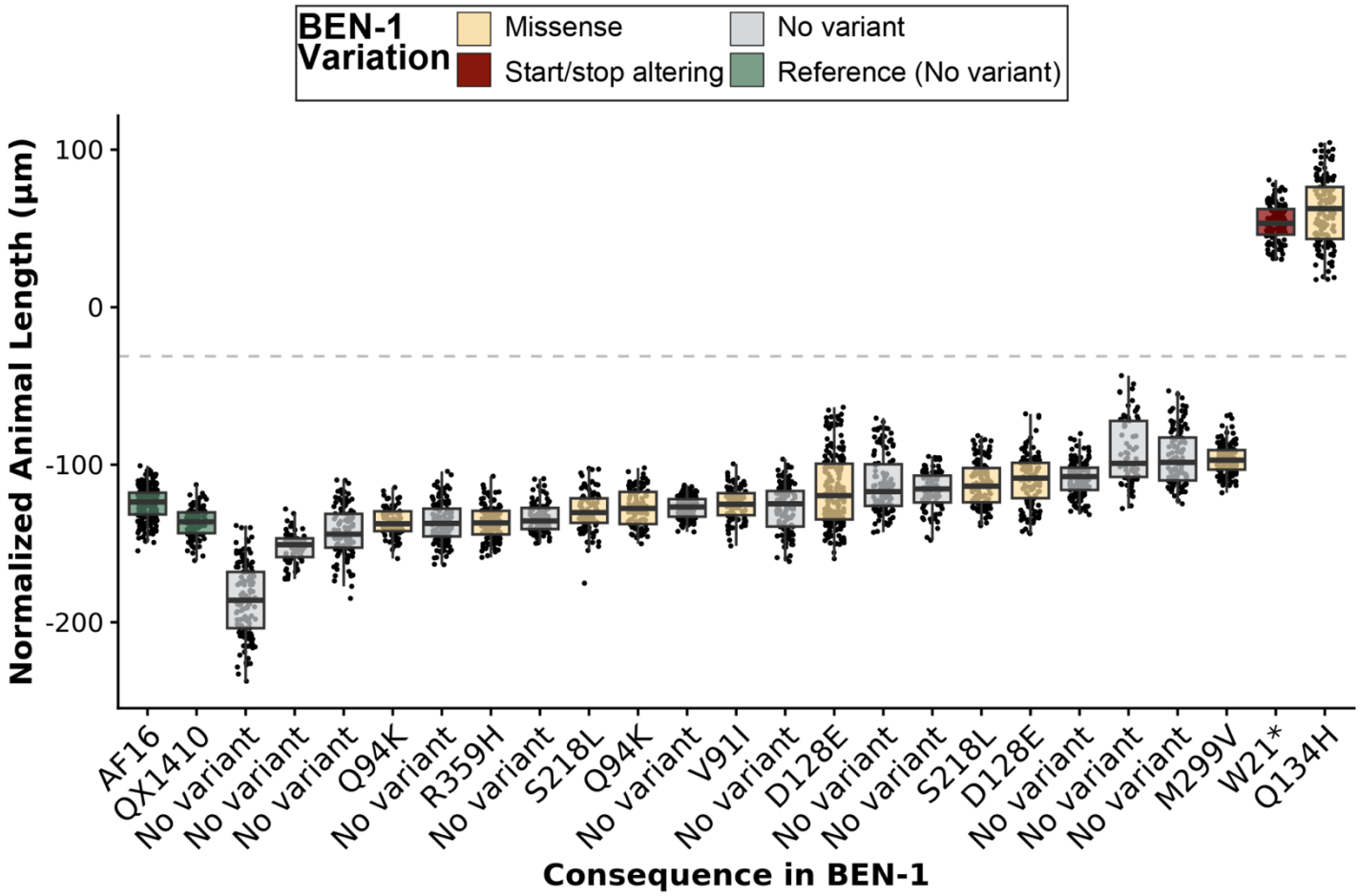

Figure 2. High-throughput assays for each *C. briggsae* strain with a high-impact variant in BEN-1 and paired predicted susceptible strains in the presence of albendazole

The regressed median animal length values for populations of nematodes grown in 30 µM albendazole (ABZ) are shown on the y-axis. Each point represents the normalized median animal length value of a well containing approximately 5-30 animals. Strains are sorted by their relative resistance to ABZ based on median animal length. Data are shown as Tukey box plots with the median as a solid horizontal line, and the top and bottom of the box representing the 75th and 25th quartiles, respectively. The top whisker is extended to the maximum point that is within the 1.5 interquartile range from the 75th quartile. The bottom whisker is extended to the minimum point that is within the 1.5 interquartile range from the 25th quartile. Strains are colored by beta-tubulin variant status. The gray dashed line marks the resistance threshold (nematode length ≥ 75% of the reference strain AF16).

466 We performed HTAs on two *C. tropicalis* predicted resistant strains with high-impact
467 variants in *Ctr*-BEN-1 (P80T and R121Q) and two predicted susceptible strains in DMSO (**S9**
468 **Figure**) and ABZ conditions. We found that both predicted resistant strains had a similar ABZ
469 response as the predicted susceptible strains, where no strains met the resistance threshold
470 (nematode length ≥ 75% of the reference strain NIC58), indicating that P80T and R121Q are not
471 associated with ABZ resistance (**Fig. 3**). These results indicate that *Ctr*-BEN-1 variants do not
472 confer ABZ resistance and that predicting ABZ resistance in *C. tropicalis* requires considering
473 factors beyond *ben-1* variation. Additionally, to evaluate if the predicted resistant variants in *Cbr*-
474 BEN-1 or *Ctr*-BEN-1 were less deleterious compared to *Cel*-BEN-1, we assessed the BLOSUM
475 and Grantham scores of each high-impact variant (Crombie et al. 2023). The BLOSUM and
476 Grantham scores measure the evolutionary likelihood of observing a particular missense
477 substitution, and we found that these scores do not accurately predict ABZ resistance (**Table S7**).
478 We performed a linear regression analysis of strain ABZ responses by the BLOSUM or Grantham
479 scores of the beta-tubulin variant in each strain. We found no significant relationship between
480 either BLOSUM or Grantham scores and ABZ response (**S10, S11, S12 Figures**). For example,
481 the only missense substitution to cause ABZ resistance in Cbr-BEN-1, Q134H, had substantially
482 less radical BLOSUM and Grantham scores (BLOSUM: 0, Grantham: 24) compared to other
483 missense substitutions, such as S218L (BLOSUM: -2, Grantham: 145).

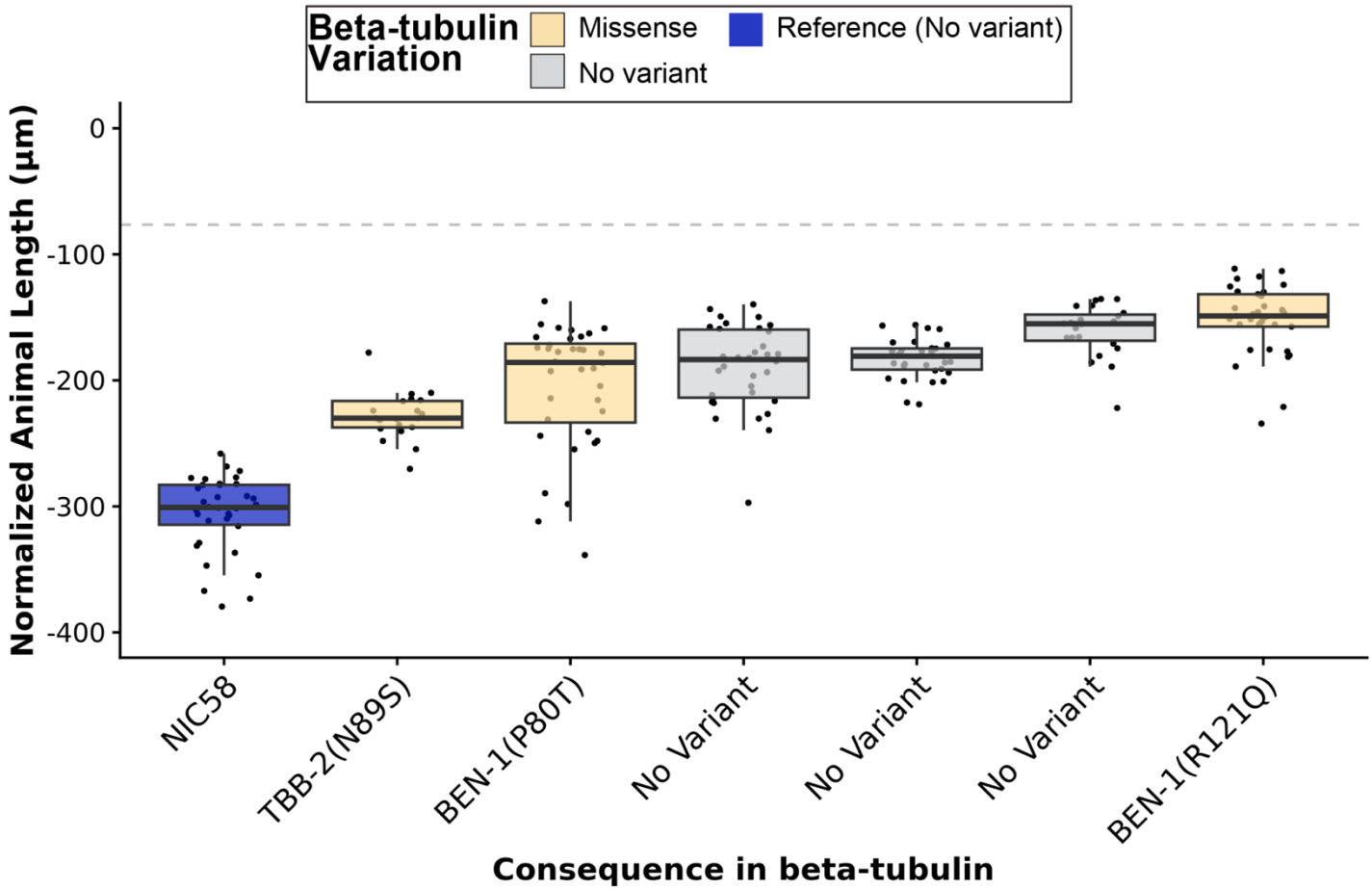

Figure 3. High-throughput assays for each *C. tropicalis* strain with a high-impact variant in BEN-1 or TBB-2 and paired predicted susceptible strains in the presence of albendazole

The regressed median animal length values for populations of nematodes grown in 30 µM albendazole (ABZ) are shown on the y-axis. Each point represents the normalized median animal length value of a well containing approximately 5-30 animals. Strains are sorted by their relative resistance to ABZ based on median animal length. Data are shown as Tukey box plots with the median as a solid horizontal line, and the top and bottom of the box representing the 75th and 25th quartiles, respectively. The top whisker is extended to the maximum point that is within the 1.5 interquartile range from the 75th quartile. The bottom whisker is extended to the minimum point that is within the 1.5 interquartile range from the 25th quartile. Strains are colored by beta-tubulin variant status. The gray dashed line marks the resistance threshold (nematode length ≥ 75% of the reference strain NIC58).

497 **3.4 Natural allelic variants in *tbb-1* and *tbb-2* are not associated with ABZ resistance across**
498 **three free-living *Caenorhabditis* species**

499 To identify if high-impact variants in other beta-tubulin genes beyond *ben-1* play a role in
500 ABZ resistance in the three free-living *Caenorhabditis* species, we categorized variants in the two
501 genes most highly expressed in *C. elegans* (*tbb-1* and *tbb-2*). Because the loss of *tbb-1* or *tbb-2*
502 is deleterious in *C. elegans* (Collins et al. 2024), LoF mutations in either gene would likely be
503 purged by purifying selection from natural populations. Therefore, as expected, we found no
504 variants in TBB-1 or TBB-2 in *C. elegans* wild strains. Unlike *C. elegans*, *C. briggsae* had four
505 missense variants in TBB-1 (T35A, V64I, A275T, and L377I) and one missense variant in TBB-2
506 (E441A). In *C. tropicalis*, we identified one rare missense variant in TBB-2 (N89S). Performing
507 the same HTA to assess nematode development as described previously, we found that none of
508 the missense variants in TBB-1 or TBB-2 in *C. briggsae* (**Fig. 4**) or *C. tropicalis* conferred ABZ
509 resistance (**Fig. 3**). These results suggest that missense variants in TBB-1 and TBB-2 are not
510 associated with ABZ resistance in *Caenorhabditis* species.

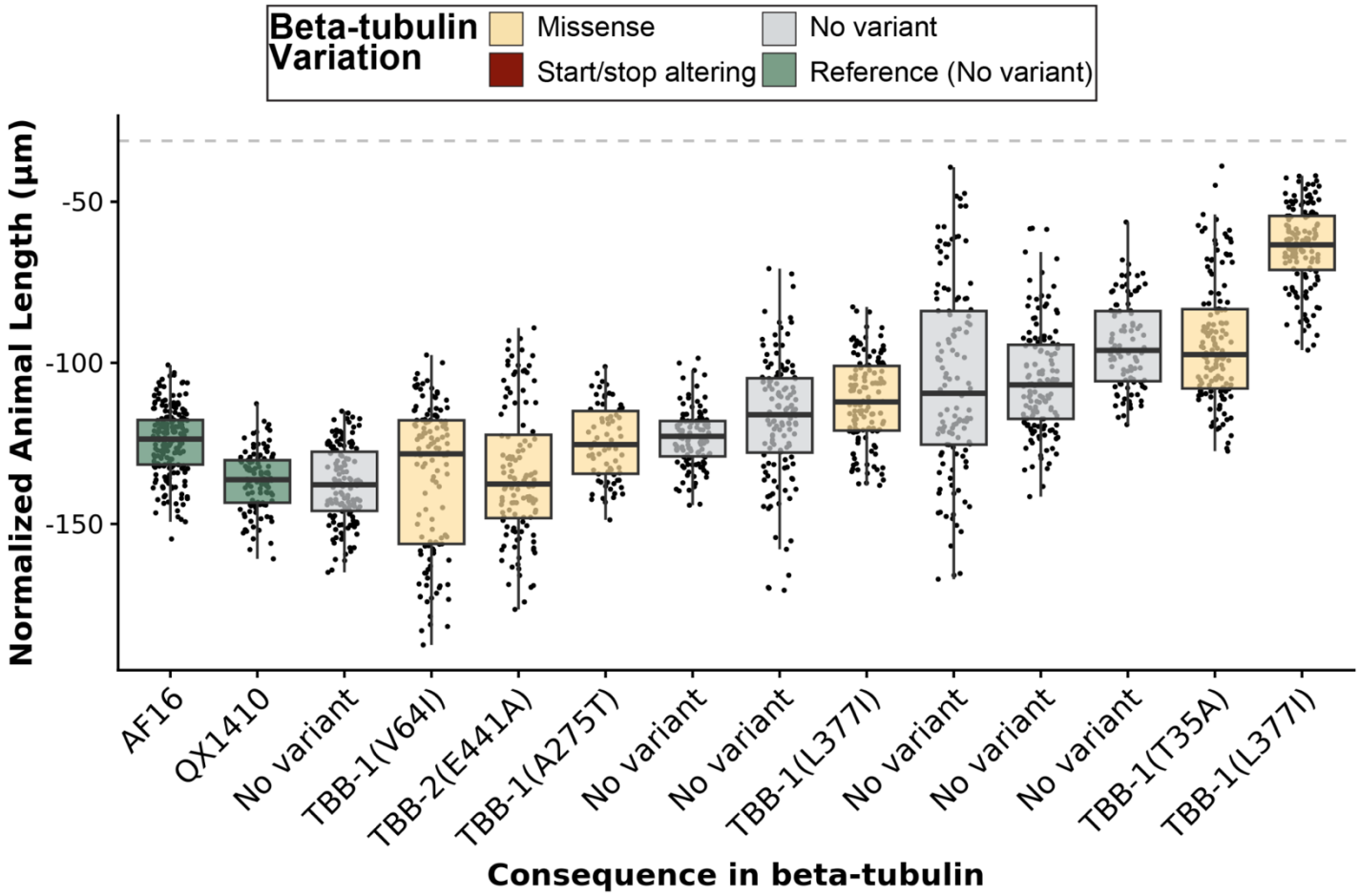

Figure 4. High-throughput assays for each *C. briggsae* strain with a high-impact variant in TBB-1 or TBB-2 in the presence of albendazole

The regressed median animal length values for populations of nematodes grown in 30 µM albendazole (ABZ) are shown on the y-axis. Each point represents the normalized median animal length value of a well containing approximately 5-30 animals. Strains are sorted by their relative resistance to ABZ based on median animal length. Data are shown as Tukey box plots with the median as a solid horizontal line, and the top and bottom of the box representing the 75th and 25th quartiles, respectively. The top whisker is extended to the maximum point that is within the 1.5 interquartile range from the 75th quartile. The bottom whisker is extended to the minimum point that is within the 1.5 interquartile range from the 25th quartile. Strains are colored by beta-tubulin variant status. The gray dashed line marks the resistance threshold (nematode length ≥ 75% of the reference strain AF16.)

523 **3.5 High-impact variants in beta-tubulin genes are rare and not enriched for geography or**
524 **substrate**

525 To better understand the evolution of BZ resistance alleles in three *Caenorhabditis*
526 species, we assessed the population-wide frequencies of each beta-tubulin consequence, along
527 with the geographic location and substrate of where each strain was isolated from nature. First,
528 to determine the prevalence of high-impact variants in the five conserved beta-tubulin genes (*tbb-*
529 *1*, *tbb-2*, *mec-7*, *tbb-4*, and *ben-1*) across *Caenorhabditis* species, we quantified the frequency of
530 each consequence (deletion, duplication, frameshift, in-frame deletion, inversion, missense,
531 splice donor, and start/stop altering) in each species. Despite extensive gobal sampling of the
532 three *Caenorhabditis* species (*C. elegans*: 611 strains, *C. briggsae*: 641 strains, *C. tropicalis*: 518
533 strains), we found that all consequences in all three *Caenorhabditis* species were rare (< 0.05%
534 of all strains in a species) (**Fig. 5**). The most variation in consequences was found in *Cel*-BEN-1,
535 where deletions, frameshifts, in-frame deletions, inversions, missense, stop/start altering variants,
536 and a duplication were found. However, we found one missense variant in *Cel*-TBB-4 and several
537 missense variants and a splice donor in *Cel*-MEC-7. *Cel-tbb-6* is unique to *C. elegans* and was
538 therefore not assessed. Overall, *C. elegans* has acquired the most diverse set of consequences
539 in BEN-1 and has conferred BZ resistance primarily by variation in *Cel-ben-1*. In *C. briggsae*, we
540 found 21 missense amino-acid substitutions and a single strain with a start/stop altering
541 consequence in *Cbr*-BEN-1. In both *Cbr*-TBB-1 and *Cbr*-TBB-2, we identified rare missense
542 consequences. Finally, we found nine strains with splice variants in *Cbr*-TBB-4 and one strain
543 with a missense variant. In *C. tropicalis*, we found missense consequences in all beta-tubulin
544 genes except *tbb-1*. These findings highlight that *C. elegans* has the most diverse set of beta-
545 tubulin variants, particularly in *ben-1*, reinforcing its role in BZ resistance.

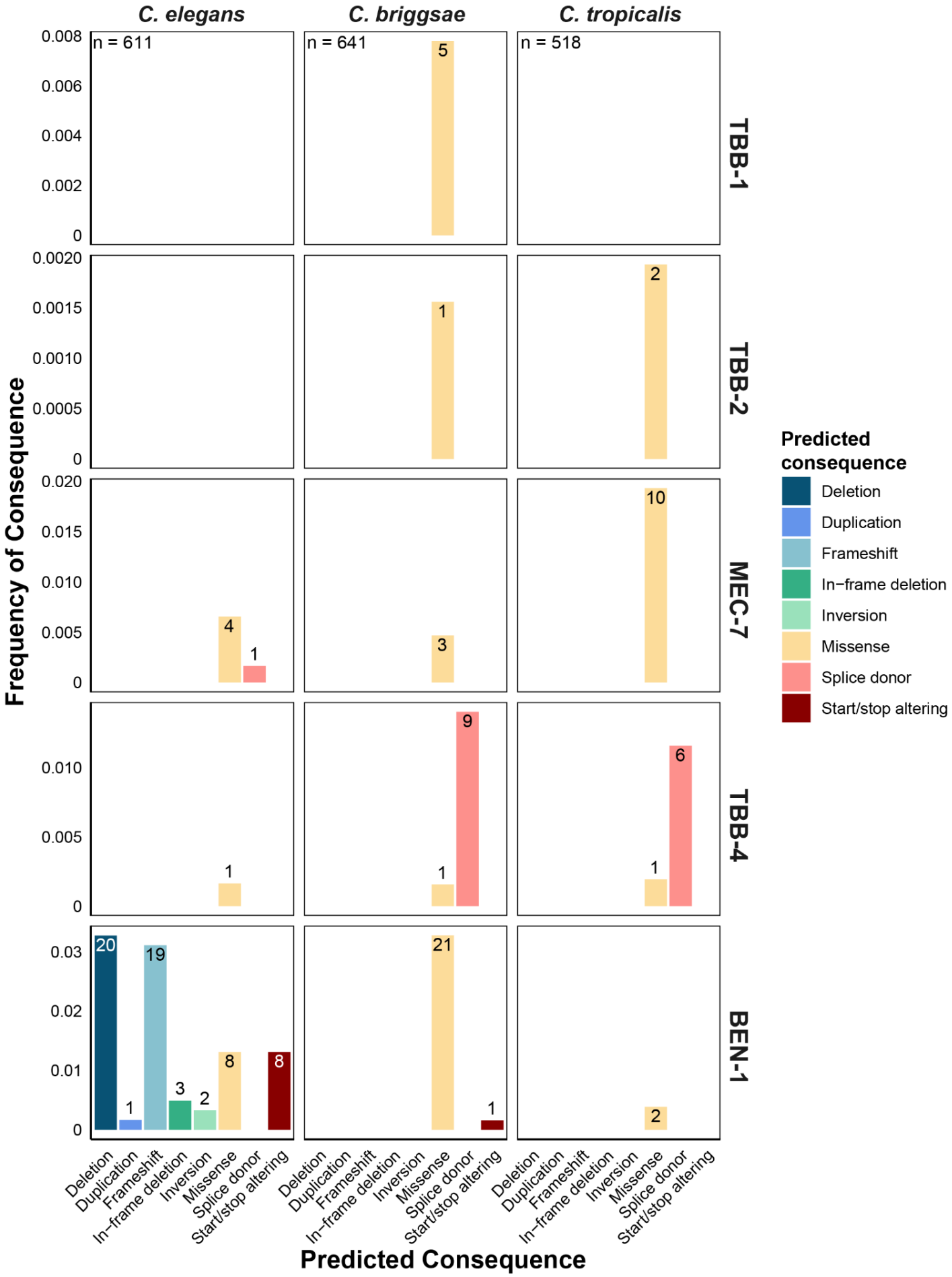
C. elegans
C. briggsae
C. tropicalis
n = 611
n = 641
n = 518
TBB-1
TBB-2
MEC-7
TBB-4
BEN-1
Frequency of Consequence
Predicted Consequence
Deletion
Duplication
Frameshift
In−frame deletion
Inversion
Missense
Splice donor
Start/stop altering
Predicted consequence

547 **Figure 5. The frequency of predicted high-impact consequences in the five beta-tubulin**
548 **genes present in natural populations of *C. elegans*, *C. briggsae*, and *C. tropicalis***
549 The frequency of SNVs present in natural populations of *C. elegans* (n = 611), *C. briggsae* (n =
550 641), and *C. tropicalis* (n = 518) (y-axis) are shown by their predicted consequence in each beta-
551 tubulin gene (x-axis). The total number of isotype reference strains with a given predicted
552 consequence are displayed on top of each bar plot.
553

554 Second, we examined the geographic distribution of strains carrying high-impact variants
555 in BEN-1, TBB-1, and TBB-2 to identify if beta-tubulin variants were associated with geography.
556 Variants in BEN-1 were found globally across the three *Caenorhabditis* species (**Fig. 6A**), with no
557 discernible geographic pattern. In *C. elegans*, variants in BEN-1 were found in more recent clades
558 (*i.e.*, strains that experienced recent selective sweeps) (Andersen et al. 2012; Zhang, Mostad,
559 and Andersen 2021) (**Fig. 6B**). *Cel*-BEN-1 variants in swept clades suggest that these mutations
560 arose as relatively recent evolutionary events and might be maintained in response to BZ-like
561 compounds in the natural niche. By contrast, in *C. briggsae*, variants in BEN-1 were distributed
562 throughout the species tree and found on more ancestral branches (*i.e.*, earlier diverged lineages
563 in the species) (**Fig. 6C**). However, it is unlikely that variants in *Cbr*-BEN-1 emerged from
564 ancestral evolutionary events, because none of the variants identified were shared across strains.
565 For *C. tropicalis*, the limited number of variants in BEN-1 precludes any definitive conclusions
566 regarding their evolutionary patterns (**Fig. 6D**). Finally, because few variants are found in TBB-1
567 and TBB-2 in *C. briggsae* and *C. tropicalis*, we cannot identify the evolutionary patterns of BZ
568 resistance in these genes (**S13 and S14 Figures**).

569 Finally, as substrates harbor distinct microbial communities that can influence the
570 evolution of BZ resistance alleles, we determined if strains carrying a high-impact variant in a
571 beta-tubulin gene were associated with specific substrates. We performed substrate enrichment
572 analysis to assess enrichment between 12 substrates and all strains in the three *Caenorhabditis*
573 species (**Table S8**). However, no significant enrichment was observed between a high-impact
574 variant in a beta-tubulin gene and any given substrate (Fisher's Exact Test, p=1) (**S15 Figure**).
575 Because no geographic or substrate enrichment was observed, evolutionary pressures driving

576 beta-tubulin variation are likely not strongly tied to substrate. Instead, it is likely that species-
577 specific evolutionary trajectories (*e.g.*, selective pressures or gene family redundancy) shape
578 differential susceptibility to BZs.

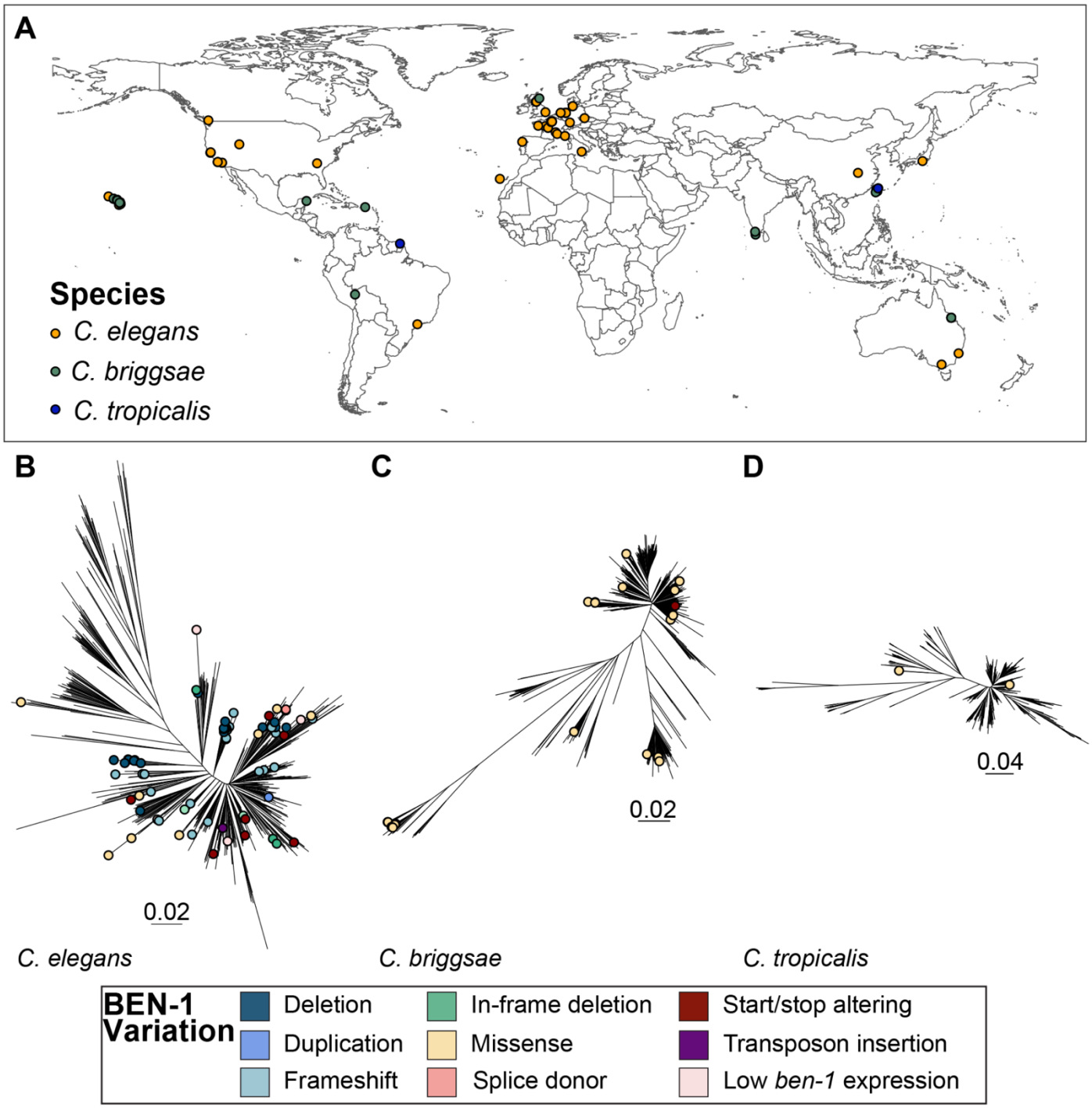

Figure 6. The global distribution of *Caenorhabditis* strains that contain predicted high-impact variation in BEN-1

(A) Each point corresponds to the sampling location of an individual *C. elegans* (orange), *C. briggsae* (green), or *C. tropicalis* (blue) isotype reference strain with a predicted high-impact consequence in BEN-1. A genome-wide phylogeny of **(B)** 611 *C. elegans*, **(C)** 641 *C. briggsae*, and **(D)** 518 *C. tropicalis* isotype reference strains where each point denotes an isotype reference strain with a predicted high-impact consequence in BEN-1 is shown.

587 **4. DISCUSSION**

588 **4.1 A lack of repeated evolution of beta-tubulin mediated BZ resistance across**
589 ***Caenorhabditis* nematodes**

590 This study provides new insights into the mechanisms of ABZ resistance across three
591 *Caenorhabditis* species. No comprehensive survey of variation in the beta-tubulin gene family or
592 BZ response had been conducted across the three *Caenorhabditis* species to date. First, we
593 found that each *Caenorhabditis* species had unique predicted high-impact beta-tubulin alleles that
594 were not shared among the three species. Next, with an expanded sampling of *C. elegans*, we
595 confirmed that a heterogeneous set of rare high-impact alleles in *ben-1* were associated with ABZ
596 resistance (Hahnel et al. 2018; Dilks et al. 2021). Additionally, we identified a heterogenous set
597 of rare high-impact alleles in *Cbr-ben-1*, but only two (W21stop and Q134H) were associated with
598 ABZ resistance. The lack of ABZ resistance associated with *Cbr-ben-1* alleles suggested that
599 other beta-tubulin genes might play a role in BZ resistance. Unlike in *C. elegans*, we identified
600 high-impact alleles in *Cbr-tbb-1* and *Cbr-tbb-2*, but alleles in these genes were not associated
601 with ABZ resistance. Finally, although we identified high-impact alleles in *ben-1*, *tbb-1*, and *tbb-2*
602 in *C. tropicalis*, we did not observe ABZ resistance. The absence of repeated evolution of ABZ
603 resistance linked to variation in beta-tubulin genes across the three *Caenorhabditis* species
604 suggests that each species either employs distinct strategies to overcome ABZ exposure,
605 possibly arising from distinct ecological niches with unique selection pressures, or they are not
606 exposed to BZ compounds in the natural niche.

607

608 **4.2 What drives the evolution of BZ resistance across *Caenorhabditis* species?**

609 The lack of shared resistance alleles among the three species highlights the complexity
610 of BZ resistance. Across clade V nematodes, BZ resistance alleles come in two types (Collins et
611 al. 2024). First, when redundant beta-tubulin genes are present, LoF alleles of a beta-tubulin gene
612 can cause resistance. Second, without redundant beta-tubulin genes, LoF alleles are

613 hypothesized to reduce fitness or even cause lethality, so only alleles that alter BZ binding cause
614 resistance. Across *Caenorhabditis* nematode species, either type could be present so additional
615 criteria must be assessed to understand the evolution of BZ resistance. We must clearly
616 determine (1) the specific role of each beta-tubulin in ABZ resistance, (2) the tissue-specific
617 expression patterns of beta-tubulins, (3) the unique selective pressures acting on each
618 *Caenorhabditis* species, and (4) non-beta-tubulin genes involved in the ABZ response.

619 In *C. elegans*, the contribution of each beta-tubulin gene to BZ response has been
620 characterized in a controlled genetic background (*i.e.*, LoF beta-tubulin alleles in the N2 strain
621 background) (Collins et al. 2024). Similarly, we must first definitively identify the role each beta-
622 tubulin gene plays in BZ resistance in *C. briggsae* and *C. tropicalis*. CRISPR-Cas9 genome
623 editing should be used to delete each beta-tubulin gene in the reference strain background of
624 each species to determine the gene's contribution to resistance. Because the reference strains
625 for *C. briggsae* (AF16 and QX1410) and *C. tropicalis* (NIC58) are sensitive to ABZ, a resistance
626 phenotype following gene deletion would confirm the role of the gene in ABZ resistance.
627 Additionally, it is possible that disrupting the function of *tbb-1* and *tbb-2* in *C. briggsae* and
628 *C. tropicalis* could be highly detrimental to animal development, as seen in *C. elegans* (Collins et
629 al. 2024). Altogether, the creation of LoF alleles will allow us to define the role each gene plays
630 on nematode fitness and BZ response, defining the likelihood that BZ resistance will evolve
631 through naturally occurring LoF alleles.

632 In *C. elegans*, significant BZ susceptibility was identified in animals that express *ben-1* in
633 cholinergic neurons, suggesting that *ben-1* function in this cell type underlies susceptibility to BZ
634 (Gibson, Ness-Cohn, and Andersen 2022). The identification of beta-tubulin specific expression
635 improves our understanding of the cellular mode of action of BZs in *C. elegans*. Similarly, we must
636 characterize the temporal and tissue-specific expression patterns of beta-tubulins in *C. briggsae*
637 and *C. tropicalis*. Tissue-specific differences in beta-tubulin expression among the three
638 *Caenorhabditis* species could influence susceptibility and the evolution of BZ resistance. To

639 compare the expression patterns of *ben-1*, *tbb-1*, and *tbb-2*, we analyzed a publicly available
640 dataset that estimated the conservation of expression between *C. elegans* and *C. briggsae*
641 orthologs in homologous cell types (Large et al. 2024). The expression patterns of *ben-1* (Jensen-
642 Shannon Distance of expression [JSDgene] = 0.21), *tbb-1* (JSDgene = 0.24), and *tbb-2* (JSDgene
643 = 0.27) were highly conserved between *C. elegans* and *C. briggsae* (Large et al. 2024), indicating
644 that these genes maintain similar transcriptional profiles across species. Lower JSD values
645 indicate higher conservation, suggesting that beta-tubulin expression is largely preserved in
646 homologous cells, which might imply that the beta-tubulins have a conserved functional role in BZ
647 response. However, the homologous cells are not cholinergic neurons, so conserved activities in
648 this specific neuronal cell type might be divergent.

649 However, some neuronal cell-types (*e.g.*, PVQ, AVD, AVJ) expressed *Cel-ben-1* at higher
650 levels than in the *Cbr-ben-1*, whereas two cell types, ADL and interior arcade cells, showed higher
651 *ben-1* expression in *C. briggsae* than in *C. elegans*. (Large et al. 2024). Therefore, differences in
652 cell-specific expression patterns of beta-tubulins might influence BZ susceptibility in each species
653 and should be further investigated. One approach involves introducing *ben-1* into a *C. briggsae*
654 *ben-1* knockout strain background using transgenesis, where multi-copy arrays express *ben-1* in
655 specific tissues, as previously done in *C. elegans* (Gibson, Ness-Cohn, and Andersen 2022).
656 Plasmids containing the coding sequence of *ben-1* are fused to tissue-specific promoters to form
657 extrachromosomal arrays in transgenic animals, allowing precise tissue-specific expression.
658 Investigating beta-tubulin expression patterns in specific tissues will clarify the role of each beta-
659 tubulin and identify the tissues that BZs target in *C. briggsae*. The same approach can be applied
660 to other beta-tubulin genes in *C. briggsae* and *C. tropicalis*. Additionally, understanding the tissue-
661 specific roles of each beta-tubulin across *Caenorhabditis* species can inform strategies for
662 managing resistance in parasitic nematodes by identifying key sites of BZ action. For instance, if
663 *ben-1* function in specific tissues is critical for BZ sensitivity, it might be possible to identify similar
664 tissues in parasitic species where beta-tubulins play a pivotal role in BZ resistance. This

665 information could lead to targeted approaches for enhancing drug efficacy, such as developing
666 treatments that specifically affect these tissues or identifying novel drug targets within them to
667 combat resistance.

668 Next, the lack of shared resistance variants across *C. elegans, C. briggsae*, and
669 *C. tropicalis* suggests that each species experiences distinct selective pressures in the evolution
670 of BZ resistance. Although *Caenorhabditis* species share overlapping niches, differences in
671 microbial communities that produce natural BZs and proximity to synthetic BZs in agriculture could
672 lead to differences in BZ response. Despite the fact that our substrate enrichment tests indicate
673 no significant association between the substrate where a strain was collected and the probability
674 of having a predicted resistance variant in a beta-tubulin gene, our broad substrate categories
675 and small number of BZ resistant *C. briggsae* and *C. tropicalis* strains might obscure finer-scale
676 ecological patterns. For instance, the microbial community composition on each substrate, such
677 as the presence or absence of BZ producing bacterial species, could shape the evolution of BZ
678 resistance. Future studies characterizing microbial communities associated with each substrate
679 might clarify the selective pressures on *Caenorhabditis* nematodes.

680 Finally, although beta-tubulins are the primary targets of BZs in Clade V nematodes, other
681 mechanisms, such as variation in detoxification pathways or drug efflux transporters, could drive
682 the evolution of BZ resistance outside the beta-tubulin gene family. In *C. elegans*, variation in BZ
683 responses among wild strains has been leveraged to identify alleles in a cytochrome P450 that
684 cause BZ resistance independent of *Cel-ben-1* (Collins et al. 2025). Similarly, variation in ABZ
685 response among *C. briggsae* and *C. tropicalis* strains can be investigated with quantitative
686 genetic mapping techniques to discover sources of variation in ABZ response among wild strains.
687 Expanding genomic resources to better characterize additional sources of variation in ABZ
688 response among wild strains (*e.g.,* SVs, transcriptomic variation) is critical to disentangle the lack
689 of repeated evolution in BZ resistance.

690 **DATA AVAILABILITY STATEMENT**

691 All code and data used to replicate the data analysis and figures are available on GitHub
692 at: https://github.com/AndersenLab/ce_cb_ct_betatubulin. Table S1 contains all beta-tubulin
693 transcript IDs in the three *Caenorhabditis* species. Tables S2, S3, and S4 contain the list of *C.*
694 *elegans*, *C. briggsae*, and *C. tropicalis* isotype strains, collection location, substrate type, and their
695 beta-tubulin variant status, respectively. Table S5 contains the manual curation of SVs found in
696 beta-tubulin genes. Table S6 contains all *C. briggsae* and *C. tropicalis* isotype strains with beta-
697 tubulin variants (*i.e.*, predicted resistant strains) and their corresponding predicted susceptible
698 strains. Table S7 contains the BLOSUM and Granthum scores for amino acid changes in the
699 beta-tubulin genes in the three *Caenorhabditis* species. Table S8 contains results from the
700 substrate enrichment analysis.

701

702 **FUNDING SOURCES**

703 Amanda O. Shaver was funded by the National Institutes of Health grant F32AI181342. Ryan
704 McKeown was supported by the National Institutes of Health Training Grant (T32 GM008449)
705 through Northwestern University's Biotechnology Training Program. This work was supported by
706 the National Institutes of Health grant R01AI153088 to ECA.

707 **CRediT AUTHOR STATEMENT**

708 **Conceptualization:** ECA

709 **Data curation:** AOS, RM

710 **Formal analysis:** AOS, RM

711 **Funding acquisition:** ECA

712 **Investigation:** AOS, JMRO

713 **Methodology:** AOS, RM

714 **Project administration:** ECA

715 **Resources:** ECA

716 **Software:** AOS, RM

717 **Supervision:** ECA

718 **Validation:** AOS

719 **Visualization:** AOS, RM

720 **Writing - original draft:** AOS

721 **Writing - reviewing & editing:** AOS, RM, ECA

722 DECLARATION OF COMPETING INTERESTS

723 The authors have declared that no competing interests exist.

724 ACKNOWLEDGEMENTS

725 We would like to thank members of the Andersen laboratory for their feedback and helpful
726 comments on this manuscript. We thank the *Caenorhabditis* Natural Diversity Resource (NSF
727 Capacity grant 2224885) for providing us with strains for this study.

728 **REFERENCES**

729 Andersen, Erik C., Joshua S. Bloom, Justin P. Gerke, and Leonid Kruglyak. 2014. "A Variant in
730 the Neuropeptide Receptor Npr-1 Is a Major Determinant of Caenorhabditis Elegans
731 Growth and Physiology." *PLoS Genetics* 10 (2): e1004156.
732 Andersen, Erik C., Justin P. Gerke, Joshua A. Shapiro, Jonathan R. Crissman, Rajarshi Ghosh,
733 Joshua S. Bloom, Marie-Anne Félix, and Leonid Kruglyak. 2012. "Chromosome-Scale
734 Selective Sweeps Shape Caenorhabditis Elegans Genomic Diversity." *Nature Genetics* 44
735 (3): 285–90.
736 Andersen, Erik C., Tyler C. Shimko, Jonathan R. Crissman, Rajarshi Ghosh, Joshua S. Bloom,
737 Hannah S. Seidel, Justin P. Gerke, and Leonid Kruglyak. 2015. "A Powerful New
738 Quantitative Genetics Platform, Combining Caenorhabditis Elegans High-Throughput
739 Fitness Assays with a Large Collection of Recombinant Strains." *G3* 5 (5): 911–20.
740 Avramenko, Russell W., Elizabeth M. Redman, Lynsey Melville, Yvonne Bartley, Janneke Wit,
741 Camila Queiroz, Dave J. Bartley, and John S. Gilleard. 2019. "Deep Amplicon Sequencing
742 as a Powerful New Tool to Screen for Sequence Polymorphisms Associated with
743 Anthelmintic Resistance in Parasitic Nematode Populations." *International Journal for*
744 *Parasitology* 49 (1): 13–26.
745 Camacho, Christiam, George Coulouris, Vahram Avagyan, Ning Ma, Jason Papadopoulos,
746 Kevin Bealer, and Thomas L. Madden. 2009. "BLAST+: Architecture and Applications."
747 *BMC Bioinformatics* 10 (1): 421.
748 Caro, Hugo, Sulyvan Dollin, Anne Biton, Bryan Brancotte, Dimitri Desvillechabrol, Yoann
749 Dufresne, Blaise Li, et al. 2023. "BioConvert: A Comprehensive Format Converter for Life
750 Sciences." *NAR Genomics and Bioinformatics* 5 (3): lqad074.
751 Cerca, José. 2023. "Understanding Natural Selection and Similarity: Convergent, Parallel and
752 Repeated Evolution." *Molecular Ecology* 32 (20): 5451–62.
753 Collins, J. B., Clayton M. Dilks, Steffen R. Hahnel, Briana Rodriguez, Bennett W. Fox, Elizabeth
754 Redman, Jingfang Yu, et al. 2025. "Naturally Occurring Variation in a Cytochrome P450
755 Modifies Thiabendazole Responses Independently of Beta-Tubulin." *PLoS Pathogens* 21
756 (1): e1012602.
757 Collins, J. B., Skyler A. Stone, Emily J. Koury, Anna G. Paredes, Fiona Shao, Crystal Lovato,
758 Michael Chen, et al. 2024. "Quantitative Tests of Albendazole Resistance in Caenorhabditis
759 Elegans Beta-Tubulin Mutants." *International Journal for Parasitology, Drugs and Drug*
760 *Resistance* 25 (August):100556.
761 Crombie, Timothy A., Ryan McKeown, Nicolas D. Moya, Kathryn S. Evans, Samuel J.
762 Widmayer, Vincent LaGrassa, Natalie Roman, et al. 2023. "CaeNDR, the Caenorhabditis
763 Natural Diversity Resource." *Nucleic Acids Research*, October.
764 https://doi.org/10.1093/nar/gkad887.
765 Danecek, Petr, James K. Bonfield, Jennifer Liddle, John Marshall, Valeriu Ohan, Martin O.
766 Pollard, Andrew Whitwham, et al. 2021. "Twelve Years of SAMtools and BCFtools."
767 *GigaScience* 10 (2). https://doi.org/10.1093/gigascience/giab008.
768 Dilks, Clayton M., Steffen R. Hahnel, Qicong Sheng, Lijiang Long, Patrick T. McGrath, and Erik
769 C. Andersen. 2020. "Quantitative Benzimidazole Resistance and Fitness Effects of
770 Parasitic Nematode Beta-Tubulin Alleles." *International Journal for Parasitology, Drugs and*
771 *Drug Resistance* 14 (December):28–36.
772 Dilks, Clayton M., Emily J. Koury, Claire M. Buchanan, and Erik C. Andersen. 2021. "Newly
773 Identified Parasitic Nematode Beta-Tubulin Alleles Confer Resistance to Benzimidazoles."
774 *International Journal for Parasitology, Drugs and Drug Resistance* 17 (December):168–75.
775 Dingerdissen, Hayley M., John Torcivia-Rodriguez, Yu Hu, Ting-Chia Chang, Raja Mazumder,
776 and Robel Kahsay. 2018. "BioMuta and BioXpress: Mutation and Expression
777 Knowledgebases for Cancer Biomarker Discovery." *Nucleic Acids Research* 46 (D1):

D1128–36.
Ghisi, Marc, Ronald Kaminsky, and Pascal Mäser. 2007. “Phenotyping and Genotyping of Haemonchus Contortus Isolates Reveals a New Putative Candidate Mutation for Benzimidazole Resistance in Nematodes.” *Veterinary Parasitology* 144 (3-4): 313–20.
Gibson, Sophia B., Elan Ness-Cohn, and Erik C. Andersen. 2022. “Benzimidazoles Cause Lethality by Inhibiting the Function of Caenorhabditis Elegans Neuronal Beta-Tubulin.” *International Journal for Parasitology, Drugs and Drug Resistance* 20 (December):89–96.
Hahnel, Dilks, Heisler, and Andersen. 2020. “Caenorhabditis Elegans in Anthelmintic research–Old Model, New Perspectives.” *International Journal for Educational and Vocational Guidance*. https://www.sciencedirect.com/science/article/pii/S2211320720300312.
Hahnel, Steffen R., Stefan Zdraljevic, Briana C. Rodriguez, Yuehui Zhao, Patrick T. McGrath, and Erik C. Andersen. 2018. “Extreme Allelic Heterogeneity at a Caenorhabditis Elegans Beta-Tubulin Locus Explains Natural Resistance to Benzimidazoles.” *PLoS Pathogens* 14 (10): e1007226.
Ireland, C. M., K. Gull, W. E. Gutteridge, and C. I. Pogson. 1979. “The Interaction of Benzimidazole Carbamates with Mammalian Microtobule Protein.” *Biochemical Pharmacology* 28 (17): 2680–82.
Kotze, A. C., J. S. Gilleard, S. R. Doyle, and R. K. Prichard. 2020. “Challenges and Opportunities for the Adoption of Molecular Diagnostics for Anthelmintic Resistance.” *International Journal of Forecasting*. https://www.sciencedirect.com/science/article/pii/S2211320720300476.
Kotze, A. C., and R. K. Prichard. 2016. “Anthelmintic Resistance in Haemonchus Contortus: History, Mechanisms and Diagnosis.” *Advances in Parasitology* 93 (March):397–428.
Kotze, Andrew C., Peter W. Hunt, Philip Skuce, Georg von Samson-Himmelstjerna, Richard J. Martin, Heinz Sager, Jürgen Krücken, et al. 2014. “Recent Advances in Candidate-Gene and Whole-Genome Approaches to the Discovery of Anthelmintic Resistance Markers and the Description of Drug/receptor Interactions.” *International Journal for Parasitology, Drugs and Drug Resistance* 4 (3): 164–84.
Krücken, Jürgen, Kira Fraundorfer, Jean Claude Mugisha, Sabrina Ramünke, Kevin C. Sifft, Dominik Geus, Felix Habarugira, et al. 2017. “Reduced Efficacy of Albendazole against Ascaris Lumbricoides in Rwandan Schoolchildren.” *International Journal for Parasitology, Drugs and Drug Resistance* 7 (3): 262–71.
Kwa, M. S., J. G. Veenstra, and M. H. Roos. 1994. “Benzimidazole Resistance in Haemonchus Contortus Is Correlated with a Conserved Mutation at Amino Acid 200 in Beta-Tubulin Isotype 1.” *Molecular and Biochemical Parasitology* 63 (2): 299–303.
Laclette, J. P., G. Guerra, and C. Zetina. 1980. “Inhibition of Tubulin Polymerization by Mebendazole.” *Biochemical and Biophysical Research Communications* 92 (2): 417–23.
Large, Christopher R. L., Rupa Khanal, Ladeana Hillier, Chau Huynh, Connor Kubo, Junhyong Kim, Robert H. Waterston, and John I. Murray. 2024. “Lineage-Resolved Analysis of Embryonic Gene Expression Evolution in C. Elegans and C. Briggsae.” *bioRxiv*. https://doi.org/10.1101/2024.02.03.578695.
Lesack, Kyle, Grace M. Mariene, Erik C. Andersen, and James D. Wasmuth. 2022. “Different Structural Variant Prediction Tools Yield Considerably Different Results in Caenorhabditis Elegans.” *PloS One* 17 (12): e0278424.
Lourdes Mottier, Maria de, and Roger K. Prichard. 2008. “Genetic Analysis of a Relationship between Macrocyclic Lactone and Benzimidazole Anthelmintic Selection on Haemonchus Contortus.” *Pharmacogenetics and Genomics* 18 (2): 129–40.
Lubega, G. W., and R. K. Prichard. 1990. “Specific Interaction of Benzimidazole Anthelmintics with Tubulin: High-Affinity Binding and Benzimidazole Resistance in Haemonchus Contortus.” *Molecular and Biochemical Parasitology* 38 (2): 221–32.
Luke, M., John Noble, Lewis Yuen, Nicolas Stevens, and Riaad Moya. 2021. “Selfing Is the

Safest Sex for Caenorhabditis Tropicalis." *eLife* 10.
Mariene, Grace M., and James D. Wasmuth. 2025. "Genome Assembly Variation and Its Implications for Gene Discovery in Nematodes." *International Journal for Parasitology*, January. https://doi.org/10.1016/j.ijpara.2025.01.004.
Mohammedsalih, Khalid M., Jürgen Krücken, Amna Khalafalla, Ahmed Bashar, Fathel-Rahman Juma, Adam Abakar, Abdalhakaim A. H. Abdalmalaik, Gerald Coles, and Georg von Samson-Himmelstjerna. 2020. "New Codon 198 β-Tubulin Polymorphisms in Highly Benzimidazole Resistant Haemonchus Contortus from Goats in Three Different States in Sudan." *Parasites & Vectors* 13 (1): 114.
Moya, Nicolas D., Lewis Stevens, Isabella R. Miller, Chloe E. Sokol, Joseph L. Galindo, Alexandra D. Bardas, Edward S. H. Koh, et al. 2023. "Novel and Improved Caenorhabditis Briggsae Gene Models Generated by Community Curation." *BMC Genomics* 24 (1): 486.
Neff, N. F., J. H. Thomas, P. Grisafi, and D. Botstein. 1983. "Isolation of the Beta-Tubulin Gene from Yeast and Demonstration of Its Essential Function in Vivo." *Cell* 33 (1): 211–19.
Noble, Luke M., John Yuen, Lewis Stevens, Nicolas Moya, Riaad Persaud, Marc Moscatelli, Jacqueline L. Jackson, et al. 2021. "Selfing Is the Safest Sex for Caenorhabditis Tropicalis." *eLife*. https://doi.org/10.7554/elife.62587.
Nyaanga, Joy, Timothy A. Crombie, Samuel J. Widmayer, and Erik C. Andersen. 2021. "easyXpress: An R Package to Analyze and Visualize High-Throughput C. Elegans Microscopy Data Generated Using CellProfiler." *PloS One* 16 (8): e0252000.
Ortiz, Edgardo M. 2019. *vcf2phylip v2.0: Convert a VCF Matrix into Several Matrix Formats for Phylogenetic Analysis*. Zenodo. https://doi.org/10.5281/ZENODO.2540861.
Pertea, Geo, and Mihaela Pertea. 2020. "GFF Utilities: GffRead and GffCompare." *F1000Research* 9 (April):304.
Qiu, Jianbo, Jianqiang Xu, Junjie Yu, Chaowei Bi, Changjun Chen, and Mingguo Zhou. 2011. "Localisation of the Benzimidazole Fungicide Binding Site of Gibberella Zeae β2-Tubulin Studied by Site-Directed Mutagenesis." *Pest Management Science* 67 (2): 191–98.
Rausch, Tobias, Thomas Zichner, Andreas Schlattl, Adrian M. Stütz, Vladimir Benes, and Jan O. Korbel. 2012. "DELLY: Structural Variant Discovery by Integrated Paired-End and Split-Read Analysis." *Bioinformatics* 28 (18): i333–39.
Roos, M. H., M. S. G. Kwa, and W. N. Grant. 1995. "New Genetic and Practical Implications of Selection for Anthelmintic Resistance in Parasitic Nematodes." *Parasitology Today (Personal Ed.)* 11 (4): 148–50.
Saitou, N., and M. Nei. 1987. "The Neighbor-Joining Method: A New Method for Reconstructing Phylogenetic Trees." *Molecular Biology and Evolution* 4 (4): 406–25.
Shaver, Amanda O., Isabella R. Miller, Etta S. Schaye, Nicolas D. Moya, J. B. Collins, Janneke Wit, Alyssa H. Blanco, et al. 2024. "Quantifying the Fitness Effects of Resistance Alleles with and without Anthelmintic Selection Pressure Using Caenorhabditis Elegans." *PLoS Pathogens* 20 (5): e1012245.
Shaver, Amanda O., Janneke Wit, Clayton M. Dilks, Timothy A. Crombie, Hanchen Li, Raffi V. Aroian, and Erik C. Andersen. 2023. "Variation in Anthelmintic Responses Are Driven by Genetic Differences among Diverse C. Elegans Wild Strains." *PLoS Pathogens* 19 (4): e1011285.
Silvestre, Anne, and Jacques Cabaret. 2002. "Mutation in Position 167 of Isotype 1 Beta-Tubulin Gene of Trichostrongylid Nematodes: Role in Benzimidazole Resistance?" *Molecular and Biochemical Parasitology* 120 (2): 297–300.
Sternberg, Paul W., Kimberly Van Auken, Qinghua Wang, Adam Wright, Karen Yook, Magdalena Zarowiecki, Valerio Arnaboldi, et al. 2024. "WormBase 2024: Status and Transitioning to Alliance Infrastructure." *Genetics* 227 (1). https://doi.org/10.1093/genetics/iyae050.
Stevens, Lewis, Nicolas D. Moya, Robyn E. Tanny, Sophia B. Gibson, Alan Tracey, Huimin Na,

880 Rojin Chitrakar, et al. 2022. “Chromosome-Level Reference Genomes for Two Strains of
881 Caenorhabditis Briggsae: An Improved Platform for Comparative Genomics.” *Genome*
882 *Biology and Evolution* 14 (4). https://doi.org/10.1093/gbe/evac042.
883 Theodorides, V. J., G. C. Scott, and M. S. Lademan. 1970. “Strains of Haemonchus Contortus
884 Resistant against Benzimidazole Anthelmintics.” *American Journal of Veterinary Research*
885 31 (5): 859–63.
886 Venkatesan, Abhinaya, Pablo D. Jimenez Castro, Arianna Morosetti, Hannah Horvath, Rebecca
887 Chen, Elizabeth Redman, Kayla Dunn, et al. 2023. “Molecular Evidence of Widespread
888 Benzimidazole Drug Resistance in Ancylostoma Caninum from Domestic Dogs throughout
889 the USA and Discovery of a Novel β-Tubulin Benzimidazole Resistance Mutation.” *PLoS*
890 *Pathogens* 19 (3): e1011146.
891 Wählby, Carolina, Lee Kamentsky, Zihan H. Liu, Tammy Riklin-Raviv, Annie L. Conery, Eyleen
892 J. O’Rourke, Katherine L. Sokolnicki, et al. 2012. “An Image Analysis Toolbox for High-
893 Throughput C. Elegans Assays.” *Nature Methods* 9 (7): 714–16.
894 Widmayer, Samuel J., Timothy A. Crombie, Joy N. Nyaanga, Kathryn S. Evans, and Erik C.
895 Andersen. 2022. “C. Elegans Toxicant Responses Vary among Genetically Diverse
896 Individuals.” *Toxicology*, August, 153292.
897 Yu, Guangchuang. 2020. “Using Ggtree to Visualize Data on Tree-Like Structures.” *Et Al*
898 *[Current Protocols in Bioinformatics]* 69 (1): e96.
899 Zamanian, Mostafa, Daniel E. Cook, Stefan Zdraljevic, Shannon C. Brady, Daehan Lee, Junho
900 Lee, and Erik C. Andersen. 2018. “Discovery of Genomic Intervals That Underlie Nematode
901 Responses to Benzimidazoles.” *PLoS Neglected Tropical Diseases* 12 (3): e0006368.
902 Zhang, Gaotian, Jake D. Mostad, and Erik C. Andersen. 2021. “Natural Variation in Fecundity Is
903 Correlated with Species-Wide Levels of Divergence in Caenorhabditis Elegans.” *G3* 11 (8).
904 https://doi.org/10.1093/g3journal/jkab168.
905 Zhang, Gaotian, Nicole M. Roberto, Daehan Lee, Steffen R. Hahnel, and Erik C. Andersen.
906 2022. “The Impact of Species-Wide Gene Expression Variation on Caenorhabditis Elegans
907 Complex Traits.” *Nature Communications* 13 (1): 3462.

908 **SUPPORTING INFORMATION**

909 **Supplemental Table 1.** Beta-tubulin transcript IDs
910 **Supplemental Table 2.** *C. elegans* isotype variant table
911 **Supplemental Table 3**. *C. briggsae* isotype variant table
912 **Supplemental Table 4.** *C. tropicalis* isotype variant table
913 **Supplemental Table 5.** Manual curation of SVs
914 **Supplemental Table 6.** *C. briggsae* and *C. tropicalis* strain pairs
915 **Supplemental Table 7.** BLOSUM and Grantham scores for amino acid changes in beta-tubulin
916 genes in the three *Caenorhabditis* species
917 **Supplemental Table 8.** Location and substrate where each isotype reference strain was
918 collected

SUPPLEMENTAL FIGURES

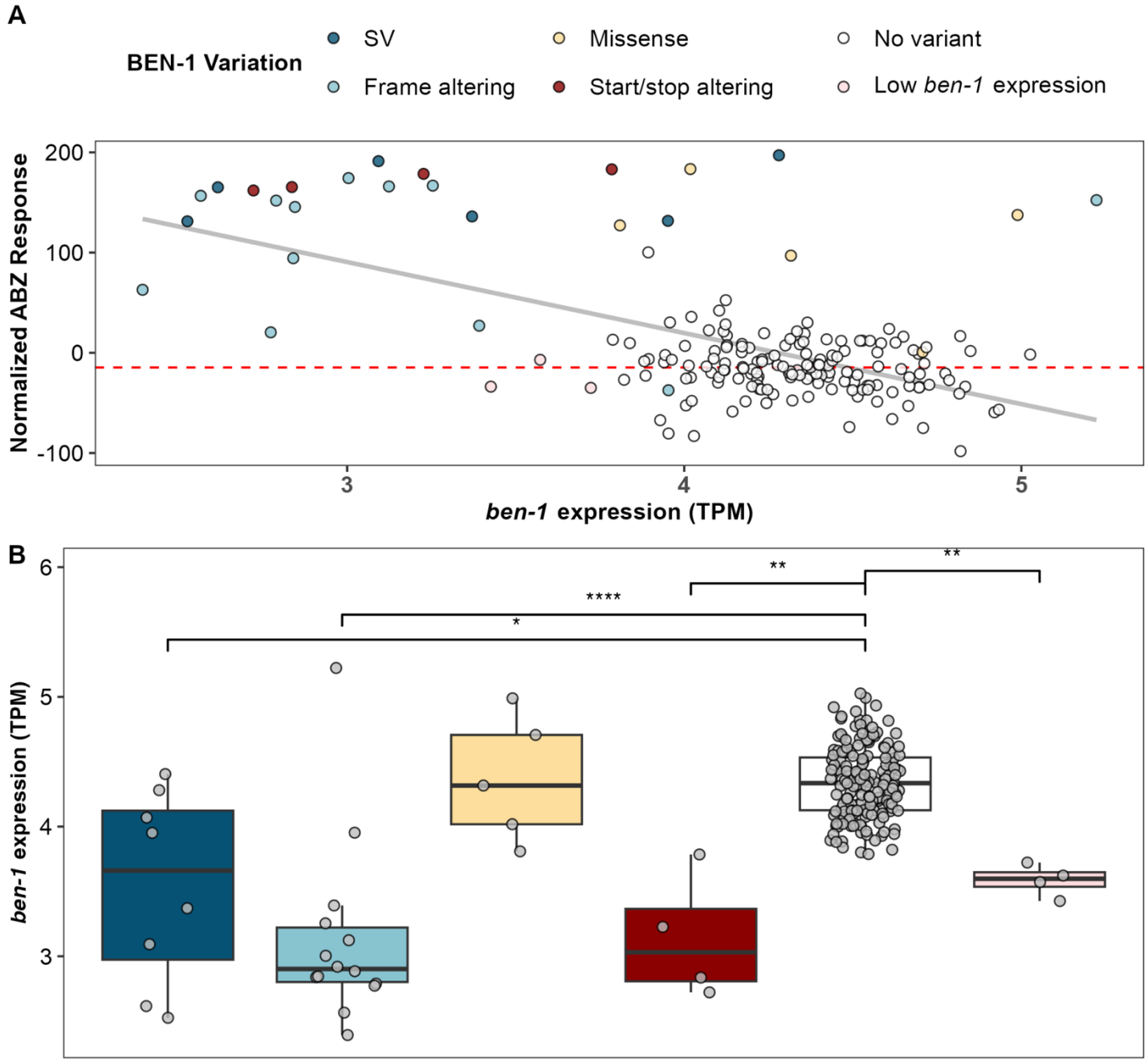

Supplemental Figure 1. The relationship between *ben-1* expression levels and albendazole response in *C. elegans* strains

(A) Scatterplot of the relationship between *ben-1* expression levels and normalized albendazole (ABZ) response across *C. elegans* wild strains. Each point represents a strain phenotyped for ABZ response in previous publications (Hahnel *et al.*, 2018; Shaver *et al.*, 2024) with *ben-1* expression data (Zhang et al. 2022)The *ben-1* expression level measured in transcripts per million (TPM) is displayed on the x-axis. The normalized ABZ response values adjusted for assay-specific effects are displayed on the y-axis. The gray line represents the linear regression fit between *ben-1* expression and normalized response (R^2 = 0.34, *p*-value = 5.16e-18), with the

linear model's coefficient of determination (R^2). Data points are colored based on the predicted functional consequence of their *ben-1* allele (*e.g.*, large structural variant (SV), Frame Altering, Missense substitution, Disrupted Start/Stop sequence, No high-impact variant, Low *ben-1* expression). A horizontal red line represents a resistance threshold calculated from the normalized phenotypes of all strains from previous publications set at 75% of the reference strain N2. Strains with normalized responses above this threshold are considered resistant to ABZ. **(B)** Boxplots of *ben-1* expression levels among individuals grouped by the predicted functional consequences of their *ben-1* alleles. Each point represents the *ben-1* expression level of an individual within each group. We tested for statistically significant differences in the expression between each consequence type and strains without a high-impact *ben-1* allele with an unpaired Wilcoxon test. Significance levels are indicated by symbols: '*' ($p < 0.05$), '**' ($p < 0.01$), '***' ($p < 0.001$), '****' ($p < 0.0001$).

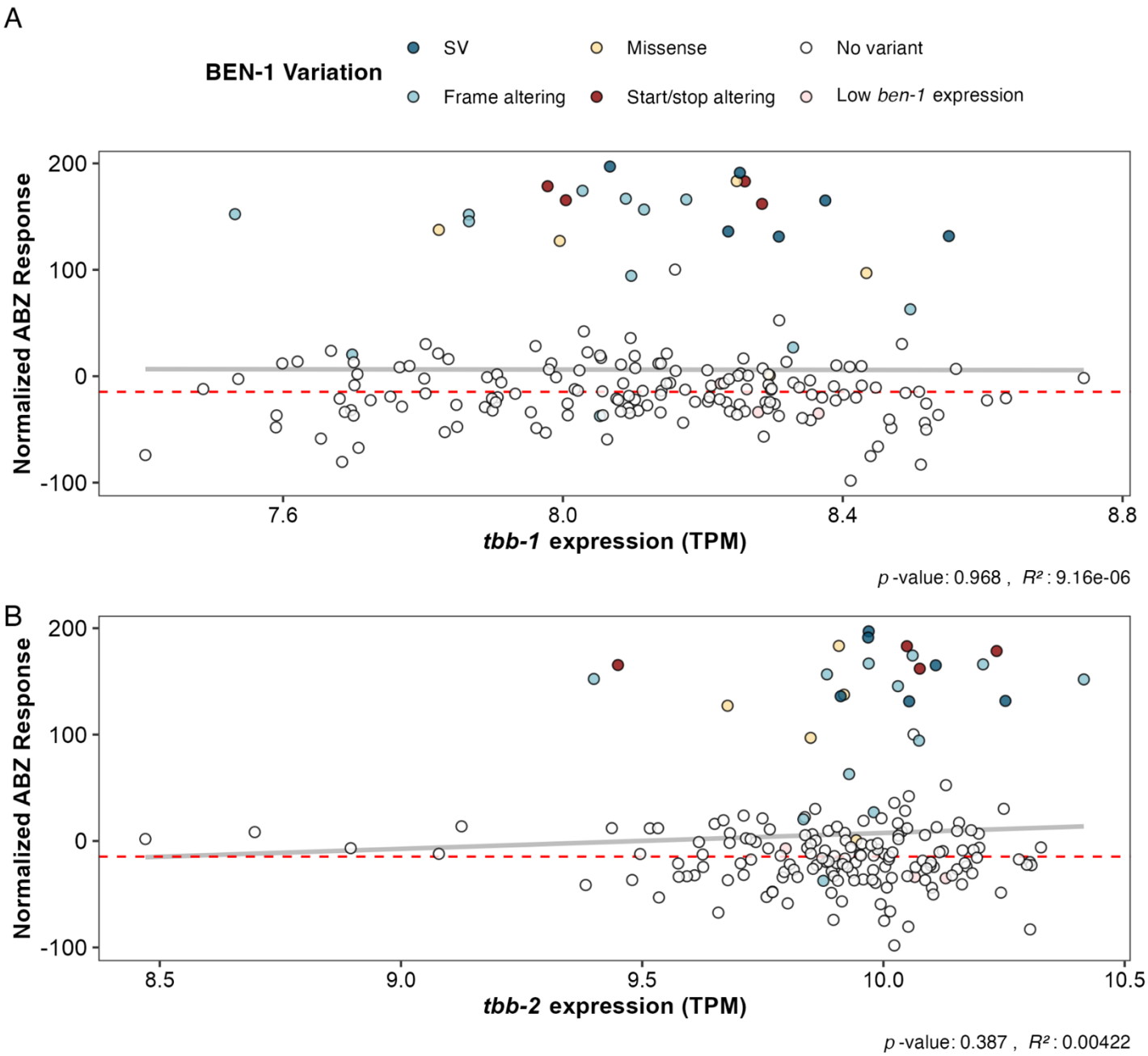

Supplemental Figure 2. The relationship between *C. elegans* beta-tubulin expression and albendazole response

Scatterplot of the relationship between **(A)** *tbb-1* and **(B)** *tbb-2* expression levels and normalized albendazole (ABZ) response across *C. elegans* wild strains. Each point represents a strain phenotyped for ABZ response in previous publications (Hahnel *et al.*, 2018; Shaver *et al.*, 2024) with *tbb-1* and *tbb-2* expression data (Zhang et al. 2022)The *tbb-1* and *tbb-2* expression levels measured in transcripts per million (TPM) are displayed on the x-axis. The normalized ABZ response values adjusted for assay-specific effects are displayed on the y-axis. The gray line represents the linear regression fit between beta-tubulin gene expression and normalized response, with the linear model's coefficient of determination (R^2). Data points are colored based

952 on the predicted functional consequence of their *ben-1* alleles (*e.g.*, large structural variant (SV),
953 Frame Altering, Missense substitution, Disrupted Start/Stop sequence, No high-impact variant,
954 Low *ben-1* expression). A horizontal red line represents a resistance threshold calculated from
955 the normalized phenotypes of all strains from previous publications set at 75% of the reference
956 strain N2. Strains with normalized responses above this threshold are considered resistant to
957 ABZ.

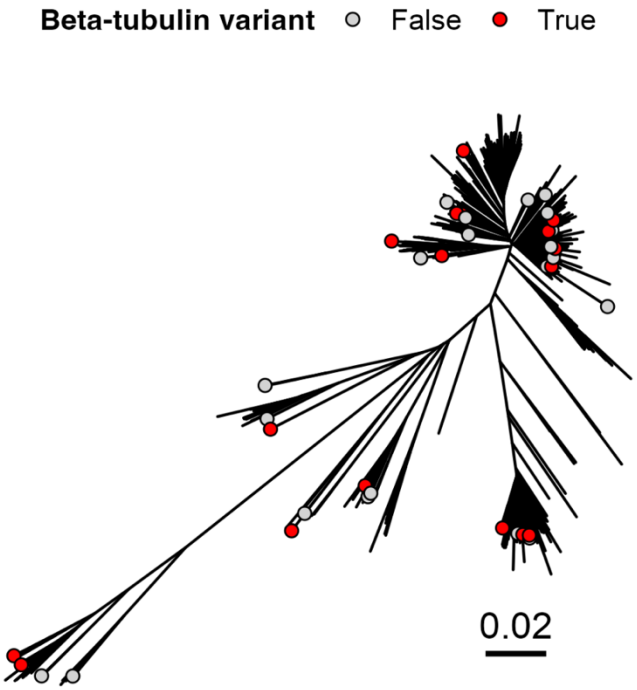

958 **Supplemental Figure 3. *C. briggsae* species tree highlighting isotype reference strains**
959 **tested for ABZ resistance.** *C. briggsae* strains with predicted high-impact variants are colored
960 red, and strains with no predicted variants in beta-tubulin genes are colored gray.

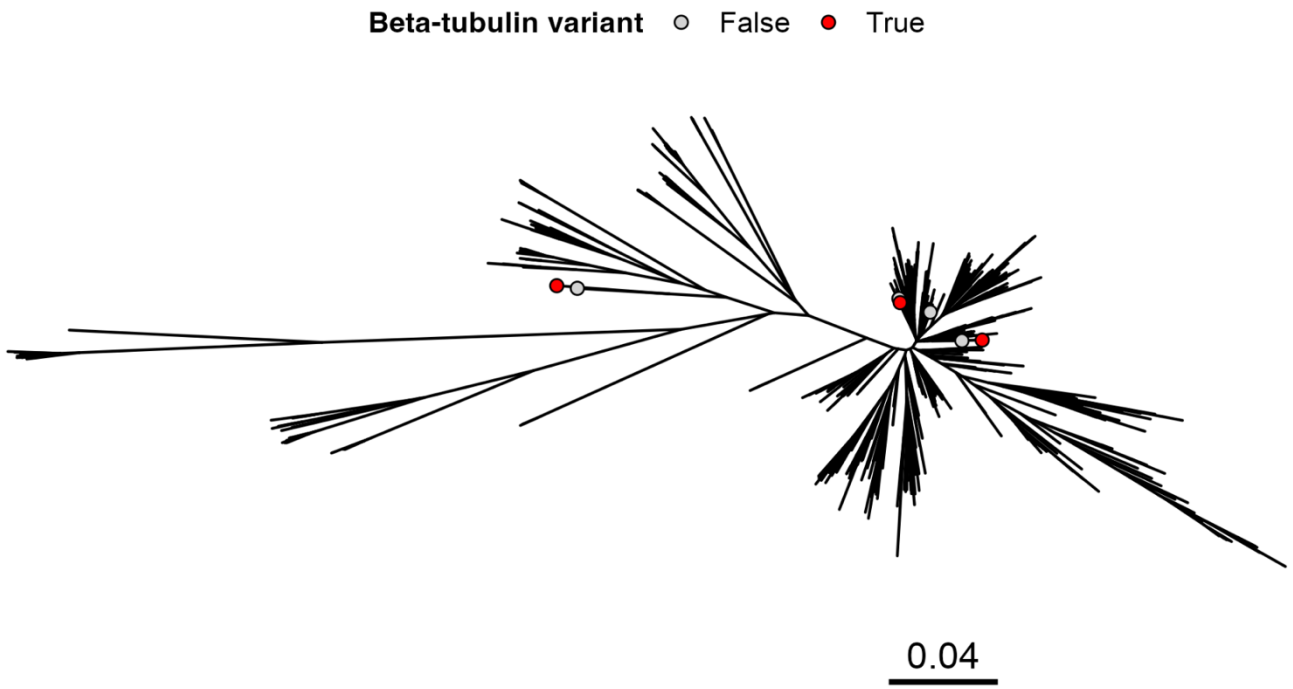

961 **Supplemental Figure 4. *C. tropicalis* species tree highlighting isotype reference strains**
962 **tested for ABZ resistance.** *C. tropicalis* strains with predicted high-impact variants are colored
963 red, and strains with no predicted variants in beta-tubulin genes are colored gray.

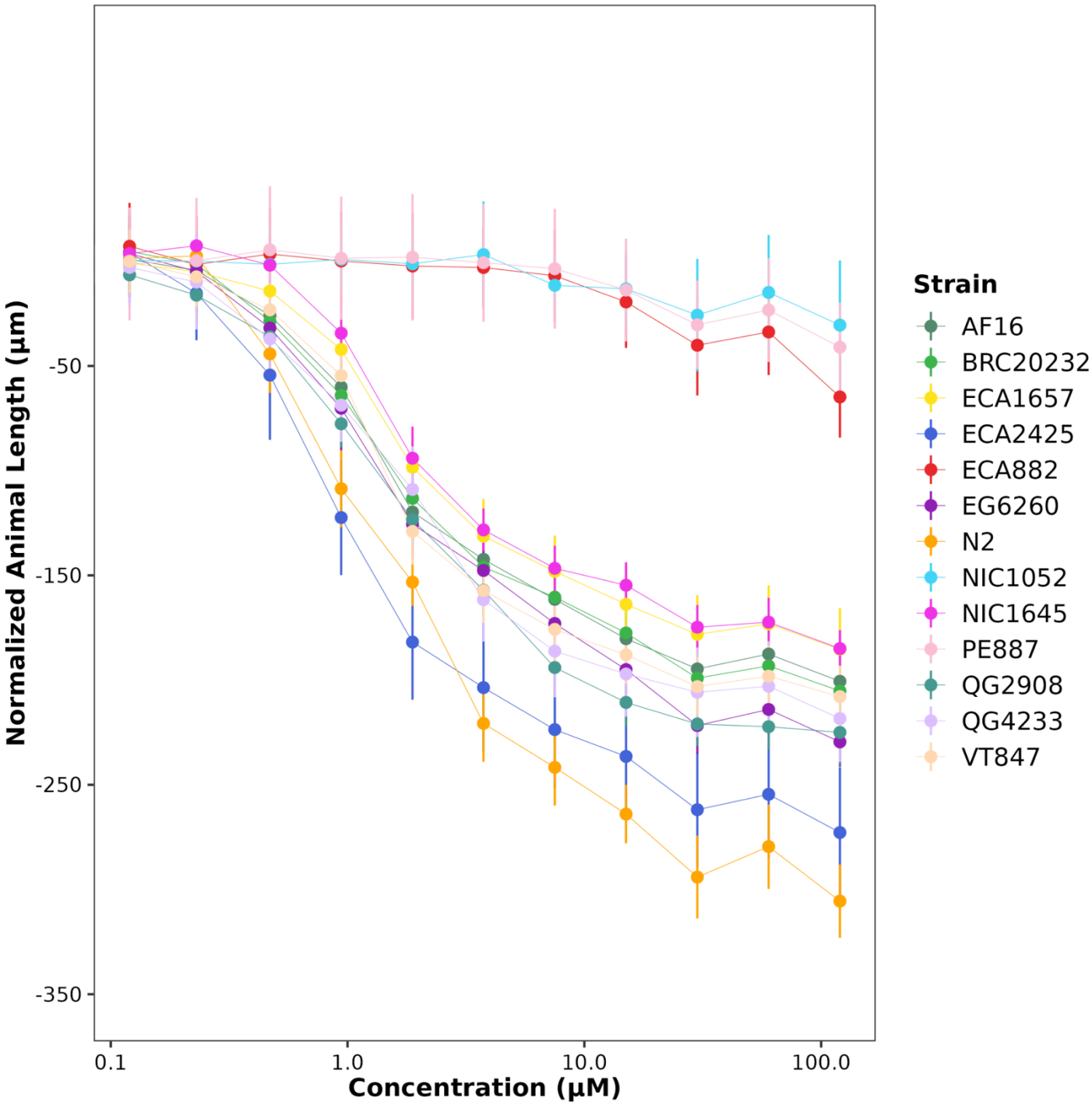

964
965 **Supplemental Figure 5. Dose-response curves for *C. briggsae* strains in albendazole**
966 Normalized animal lengths (y-axis) are plotted for each strain as a function of the dose of
967 albendazole (ABZ) in the high-throughput development assay (x-axis). Strains are denoted by
968 color. Lines extending vertically from points represent the standard deviation from the mean
969 response. Statistical normalization of animal lengths is described in *Methods*. *C. elegans* strains
970 N2 and ECA882 were added for ABZ-susceptible and ABZ-resistant controls, respectively.
971

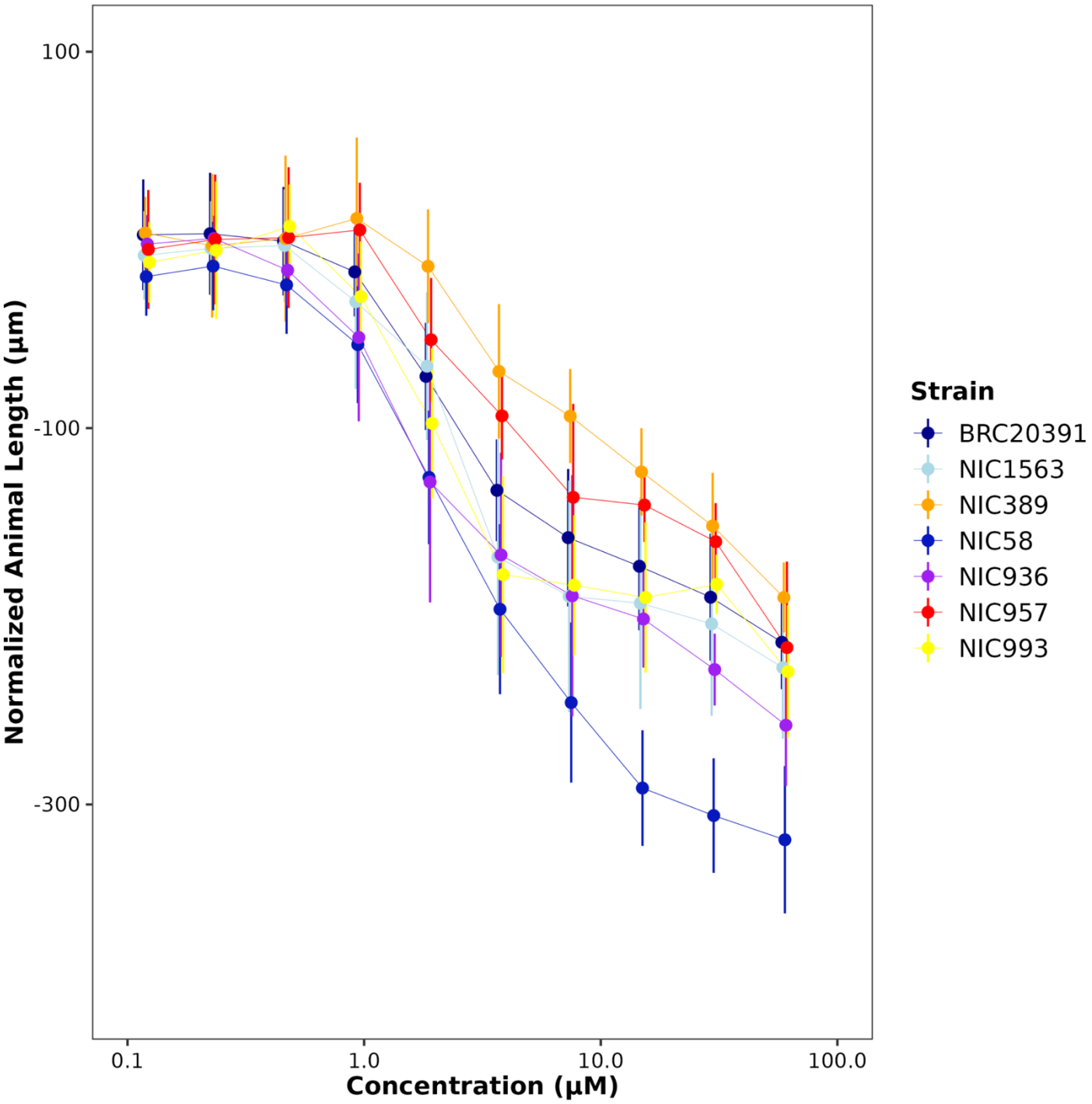

Supplemental Figure 6. Dose-response curves for *C. tropicalis* strains in albendazole
Normalized animal lengths (y-axis) are plotted for each strain as a function of the dose of albendazole (ABZ) in the high-throughput development assay (x-axis). Strains are denoted by color. Lines extending vertically from points represent the standard deviation from the mean response. Statistical normalization of animal lengths is described in *Methods*.

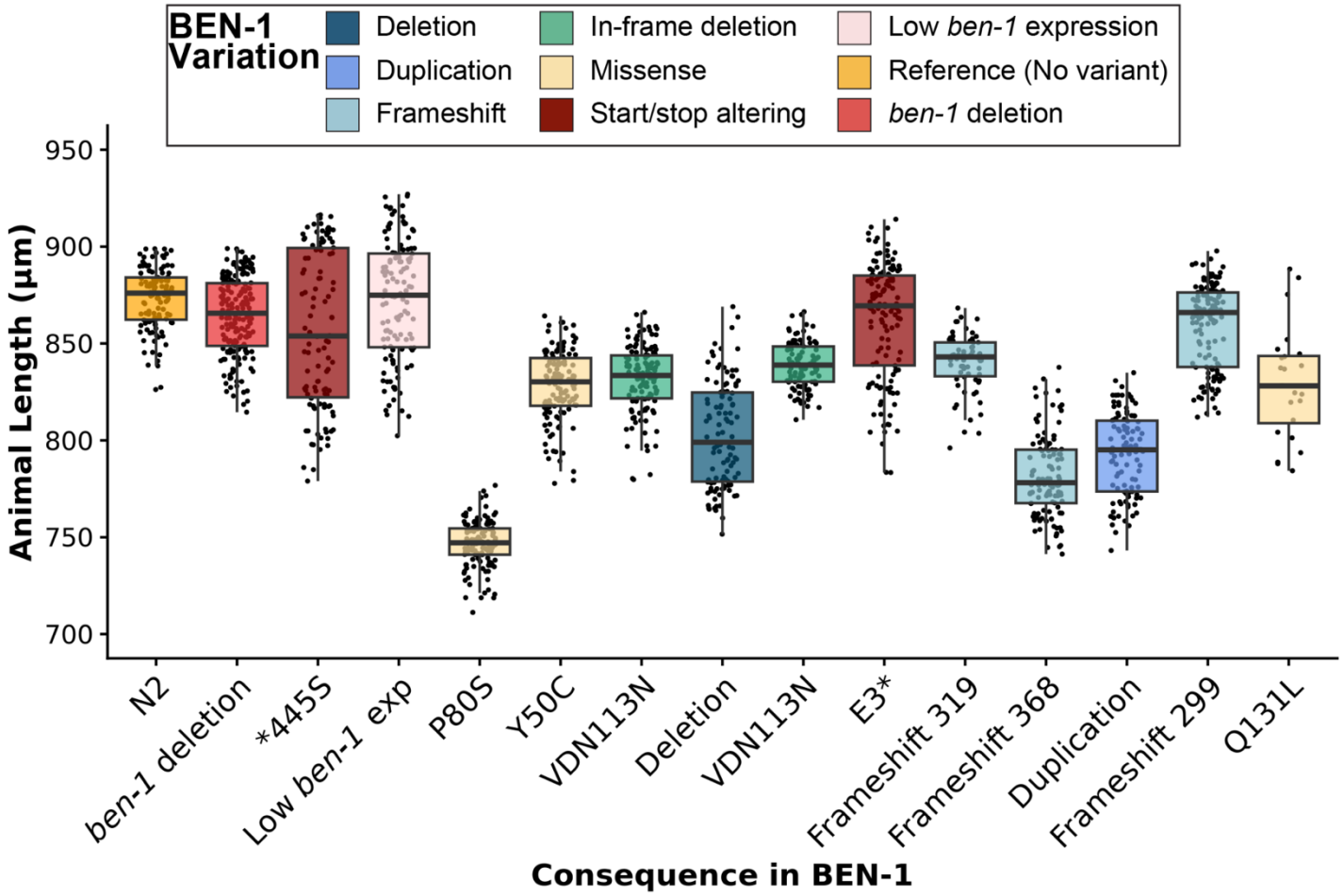

Supplemental Figure 7. High-throughput assays for each *C. elegans* strain in control conditions

Median animal length values from populations of nematodes grown in DMSO are shown on the y-axis. Each point represents the median animal length from a well containing approximately 5-30 animals. Data are shown as Tukey box plots with the median as a solid horizontal line, the top and bottom of the box representing the 75th and 25th quartiles, respectively. The top whisker is extended to the maximum point that is within a 1.5 interquartile range from the 75th quartile. The bottom whisker is extended to the minimum point that is within the 1.5 interquartile range from the 25th quartile.

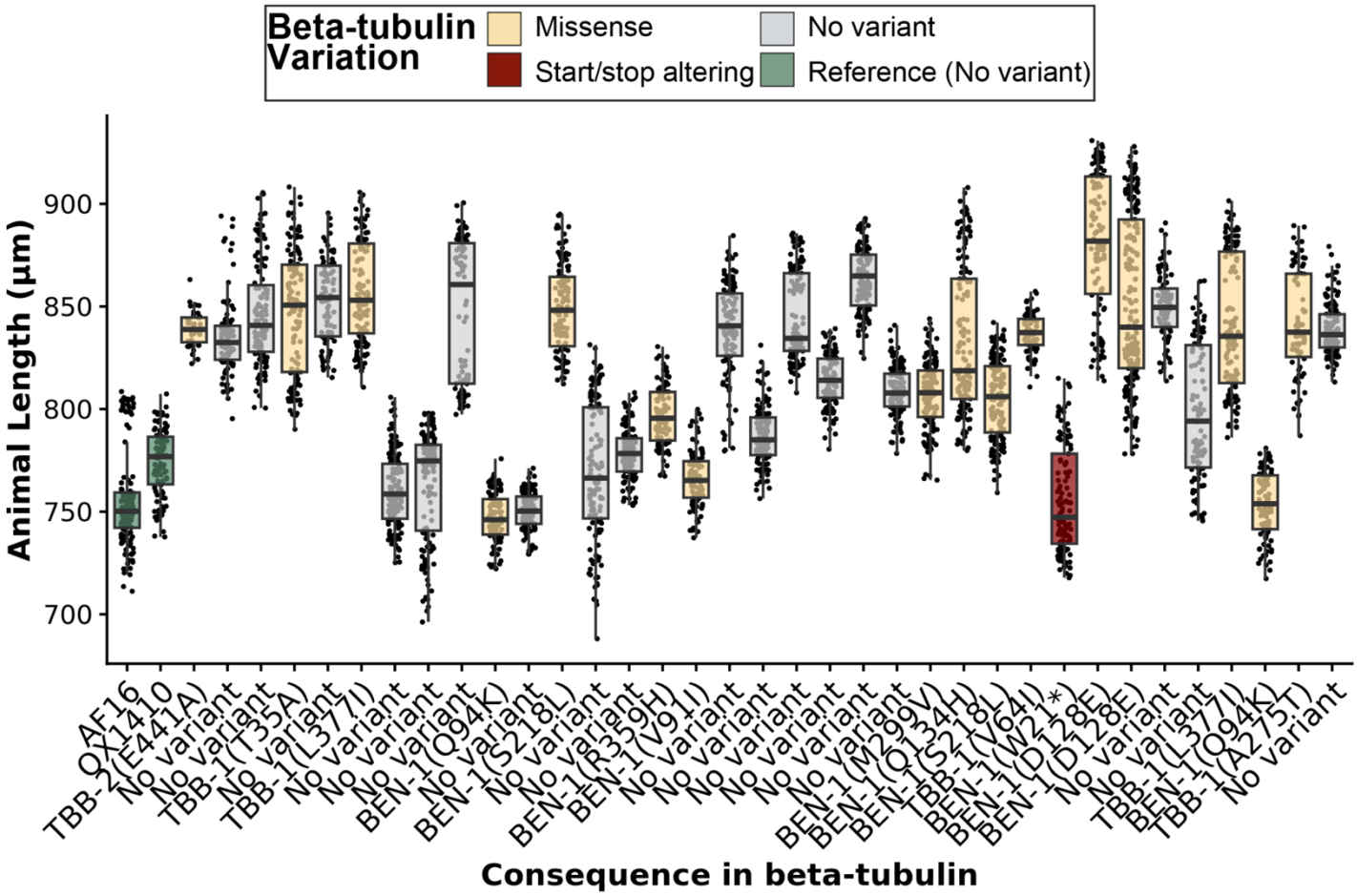

Supplemental Figure 8. High-throughput assays for each *C. briggsae* strain in control conditions.
Median animal length values from populations of nematodes grown in DMSO are shown on the y-axis. Each point represents the median animal length from a well containing approximately 5-30 animals. Data are shown as Tukey box plots with the median as a solid horizontal line, the top and bottom of the box representing the 75th and 25th quartiles, respectively. The top whisker is extended to the maximum point that is within a 1.5 interquartile range from the 75th quartile. The bottom whisker is extended to the minimum point that is within the 1.5 interquartile range from the 25th quartile. Strains are colored by beta-tubulin variant status.

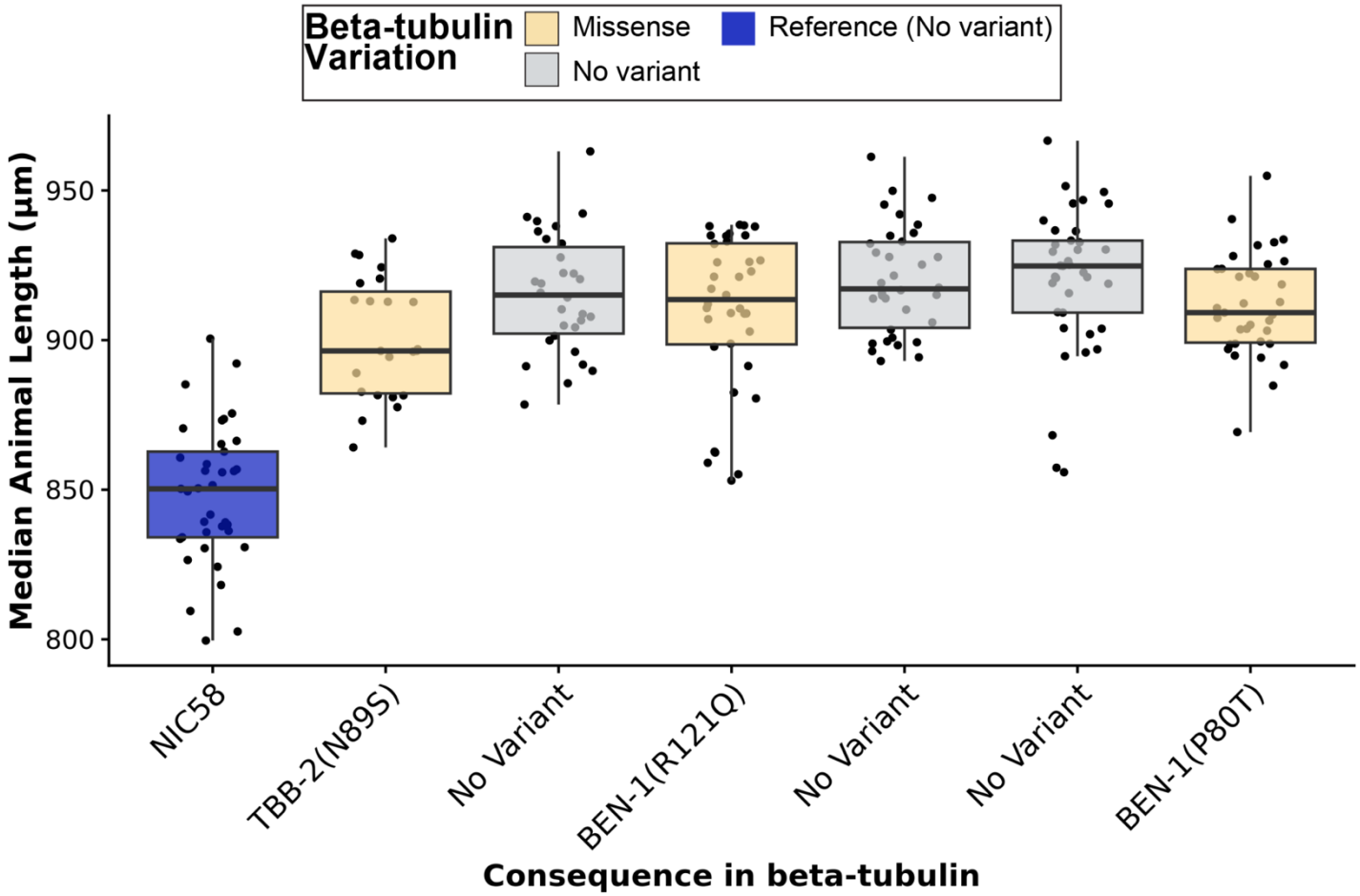

Supplemental Figure 9. High-throughput assays for each *C. tropicalis* strain in control conditions

Median animal length values from populations of nematodes grown in DMSO are shown on the y-axis. Each point represents the median animal length from a well containing approximately 5-30 animals. Data are shown as Tukey box plots with the median as a solid horizontal line, the top and bottom of the box representing the 75th and 25th quartiles, respectively. The top whisker is extended to the maximum point that is within a 1.5 interquartile range from the 75th quartile. The bottom whisker is extended to the minimum point that is within the 1.5 interquartile range from the 25th quartile. Strains are colored by beta-tubulin variant status.

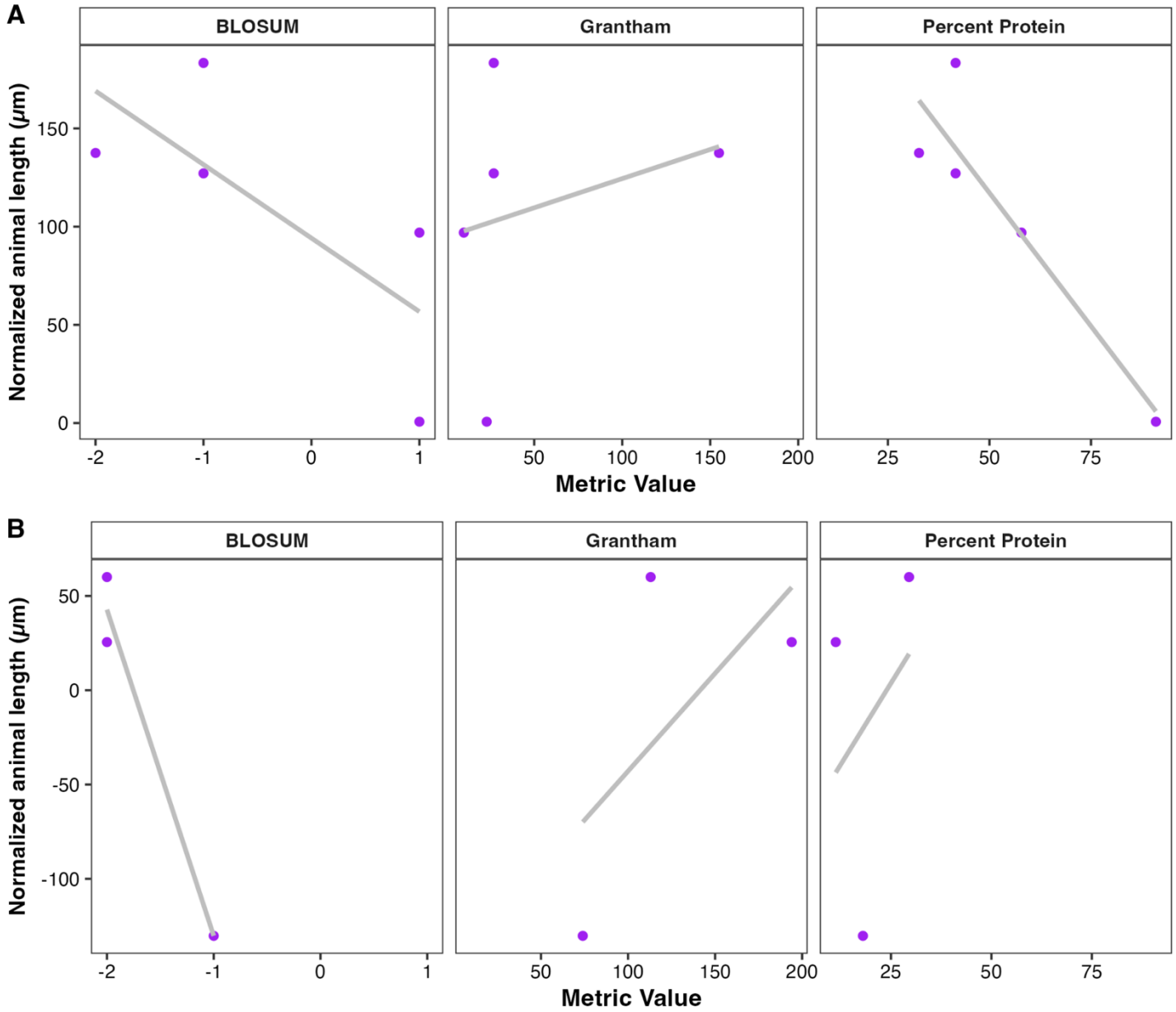

Supplemental Figure 10. Relationship between missense substitutions in BEN-1 and albendazole response in *C. elegans* strains. Scatterplots show the relationship between normalized median animal length (y-axis) and three amino acid substitution scoring metrics (x-axis): BLOSUM (R^2 = 0.97, *p*-value = 0.11), Grantham (R^2 = 0.39, *p*-value = 0.57), and percent protein (R^2 = 0.1, *p*-value = 0.8). Each point represents a *C. elegans* strain with a missense substitution in BEN-1 that was **(A)** phenotyped for ABZ response inprevious assays (Hahnel et al. 2018; Shaver et al. 2024) or **(B)** in the high-throughput assays performed for this manuscript are reported. Gray lines indicate the linear regression fit for these models.

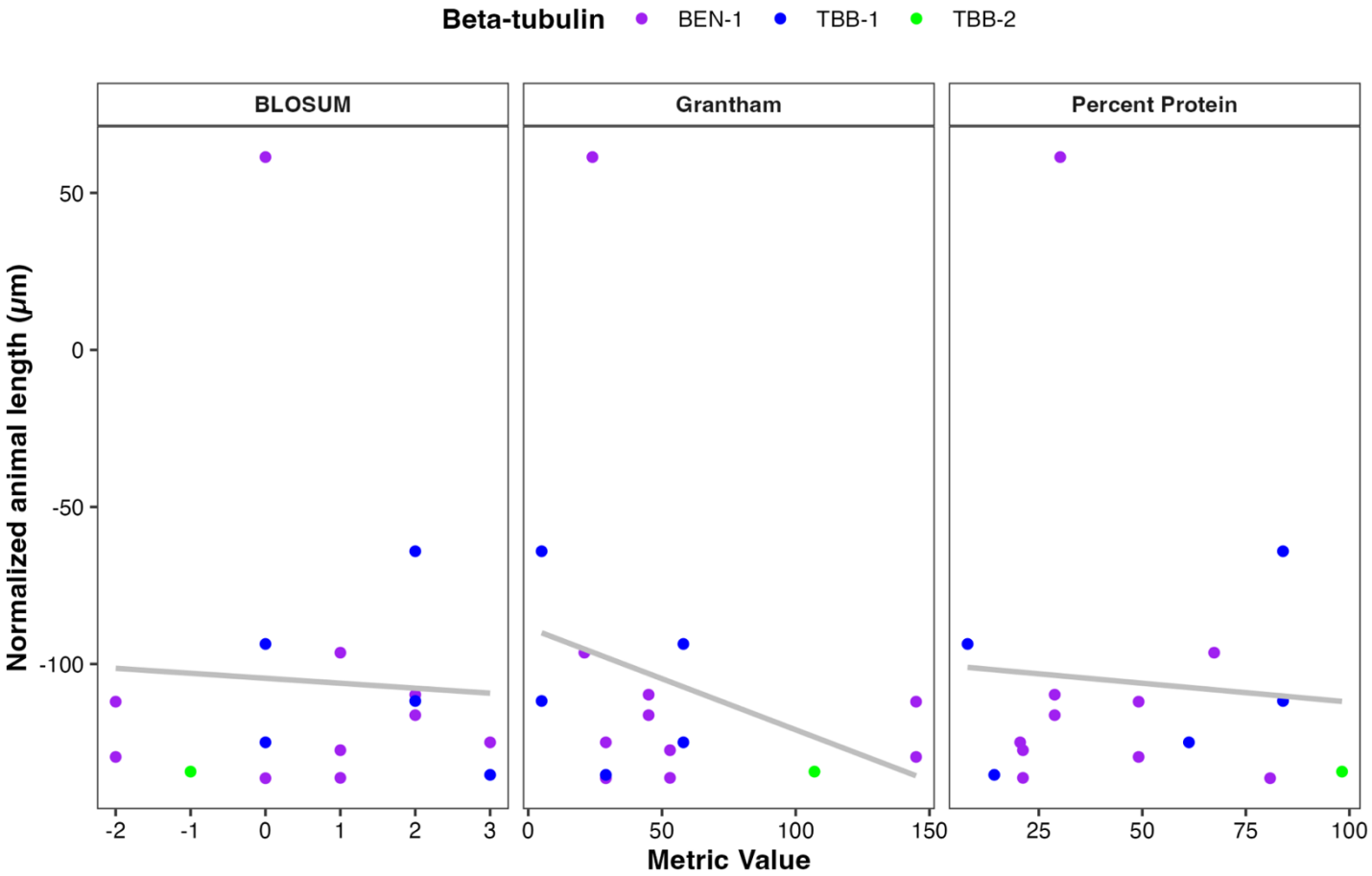

1017 **Supplemental Figure 11. Relationship between missense substitutions in BEN-1, TBB-1,**
1018 **TBB-2 and albendazole response in *C. briggsae* strains.** Scatterplots show the relationship
1019 between normalized median animal length (y-axis) and three amino acid substitution scoring
1020 metrics (x-axis): BLOSUM (R^2 = 0.0, *p*-value = 0.85), Grantham (R^2 = 0.08, *p*-value = 0.28),
1021 percent protein (R^2 = 0.01, *p*-value = 0.79). Each point represents a *C. briggsae* strain with a
1022 missense substitution in either BEN-1, TBB-1, or TBB-2. Gray lines indicate the linear regression
1023 fit, and the R^2 and *p*-values of these models are displayed in each panel

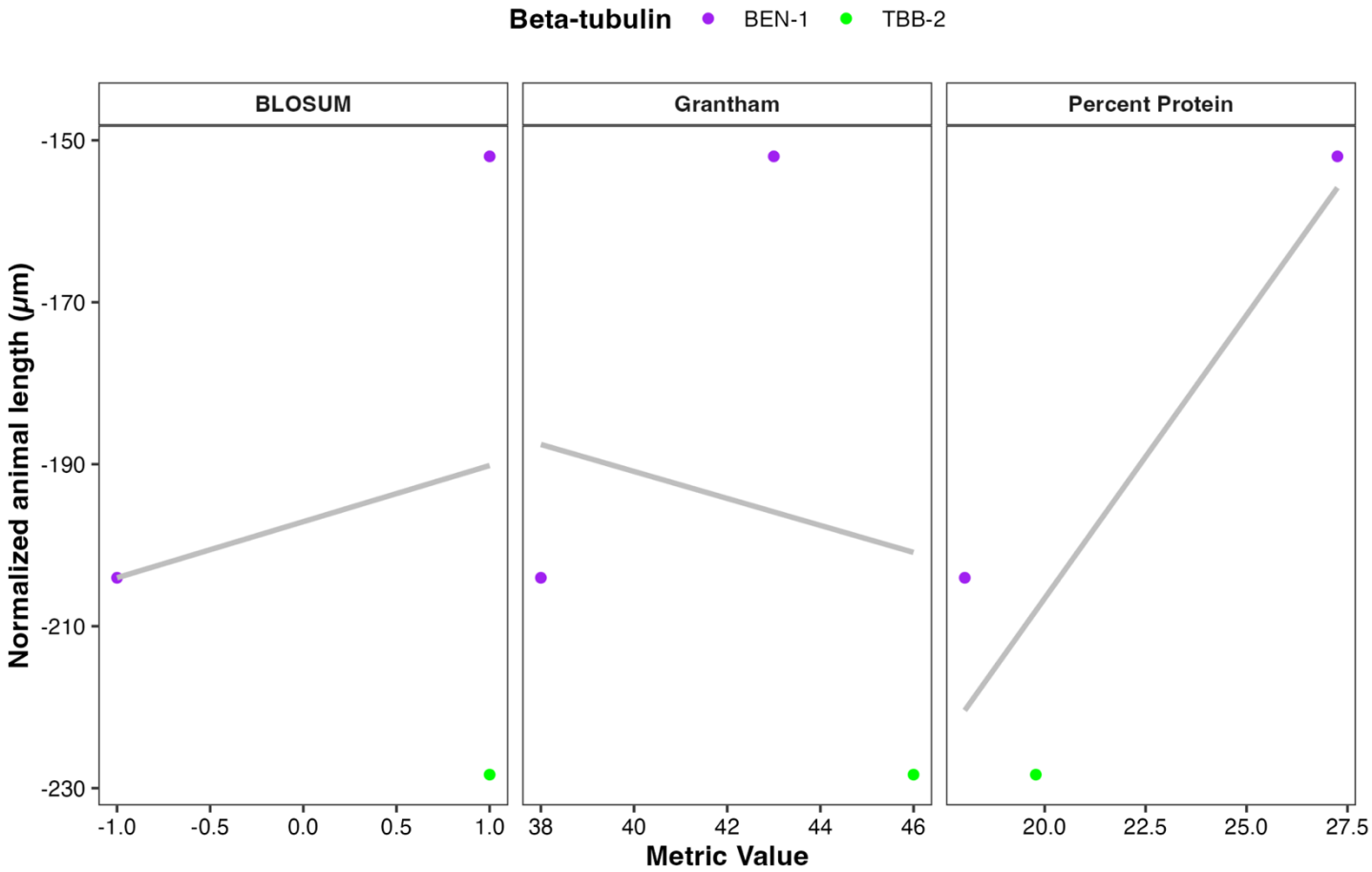

Supplemental Figure 12. Relationship between missense substitutions in BEN-1 or TBB-2 and albendazole response in *C. tropicalis* strains. Scatterplots show the relationship between normalized median animal length (y-axis) and three amino acid substitution scoring metrics (x-axis): BLOSUM (R^2 = 0.04, *p*-value = 0.87), Grantham (R^2 = 0.03, *p*-value = 0.89), percent protein (R^2 = 0.77, *p*-value = 0.32). Each point represents a *C. tropicalis* strain with a missense substitution in BEN-1 or TBB-2. Gray lines indicate the linear regression fit of these models.

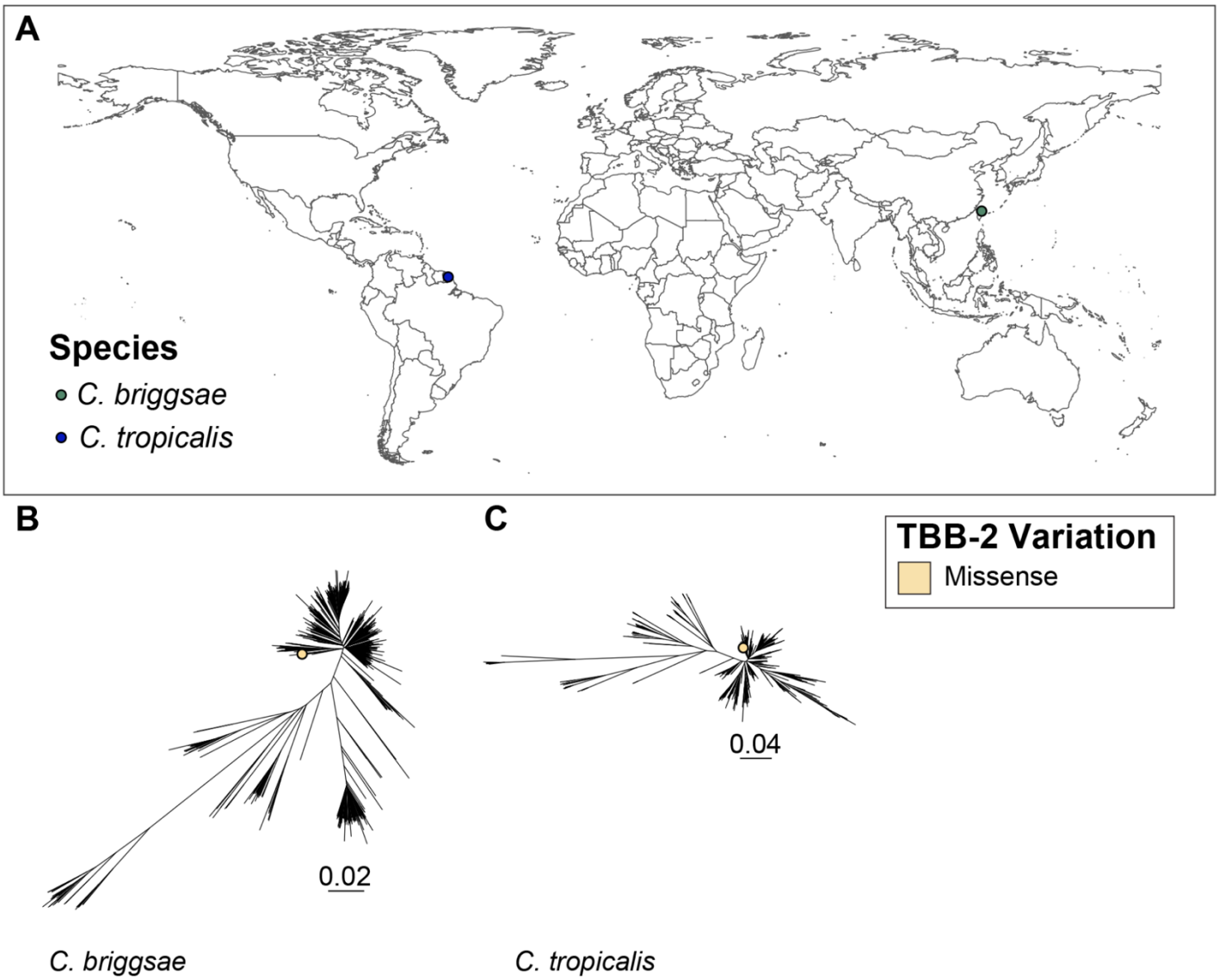

Supplemental Figure 13. The global distribution of *Caenorhabditis* strains that contain predicted high-impact variation in *tbb-2*
(A) Each point corresponds to the sampling location of an individual *C. briggsae* or *C. tropicalis* isotype reference strain with a predicted high-impact consequence in the gene *tbb-2*. A genome-wide phylogeny of **(B)** 641 *C. briggsae* and **(C)** 518 *C. tropicalis* isotype reference strains where each point denotes an isotype reference strain with a predicted high-impact consequence in *tbb-2*.

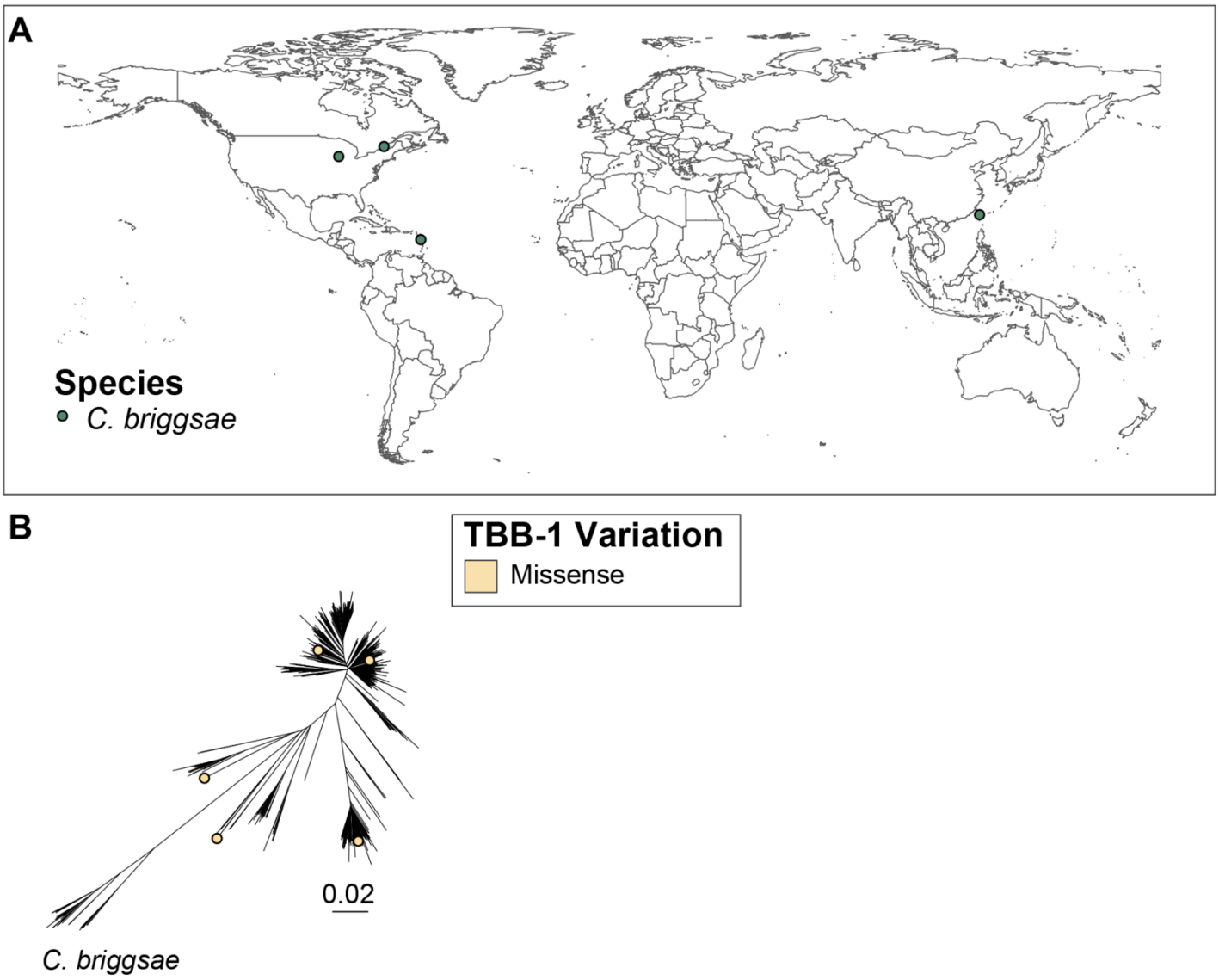

1037
1038 **Supplemental Figure 14. The global distribution of *Caenorhabditis* strains that contain**
1039 **predicted high-impact variation in *tbb-1***
1040 **(A)** Each point corresponds to the sampling location of an individual *C. briggsae* or *C. tropicalis*
1041 isotype reference strain with a predicted high-impact consequence in the gene *tbb-1*. **(B)** A
1042 genome-wide phylogeny of 641 *C. briggsae* isotype reference strains where each point denotes
1043 an isotype reference strain with a predicted high-impact consequence in *tbb-1*. One isotype,
1044 XZ1213 has a high-impact *tbb-1* variant, but sampling coordinates were not recorded. **(C)** A
1045 genome-wide phylogeny of 518 *C. tropicalis* isotype reference strains where each point denotes
1046 an isotype reference strain with a predicted high-impact consequence in *tbb-1*.

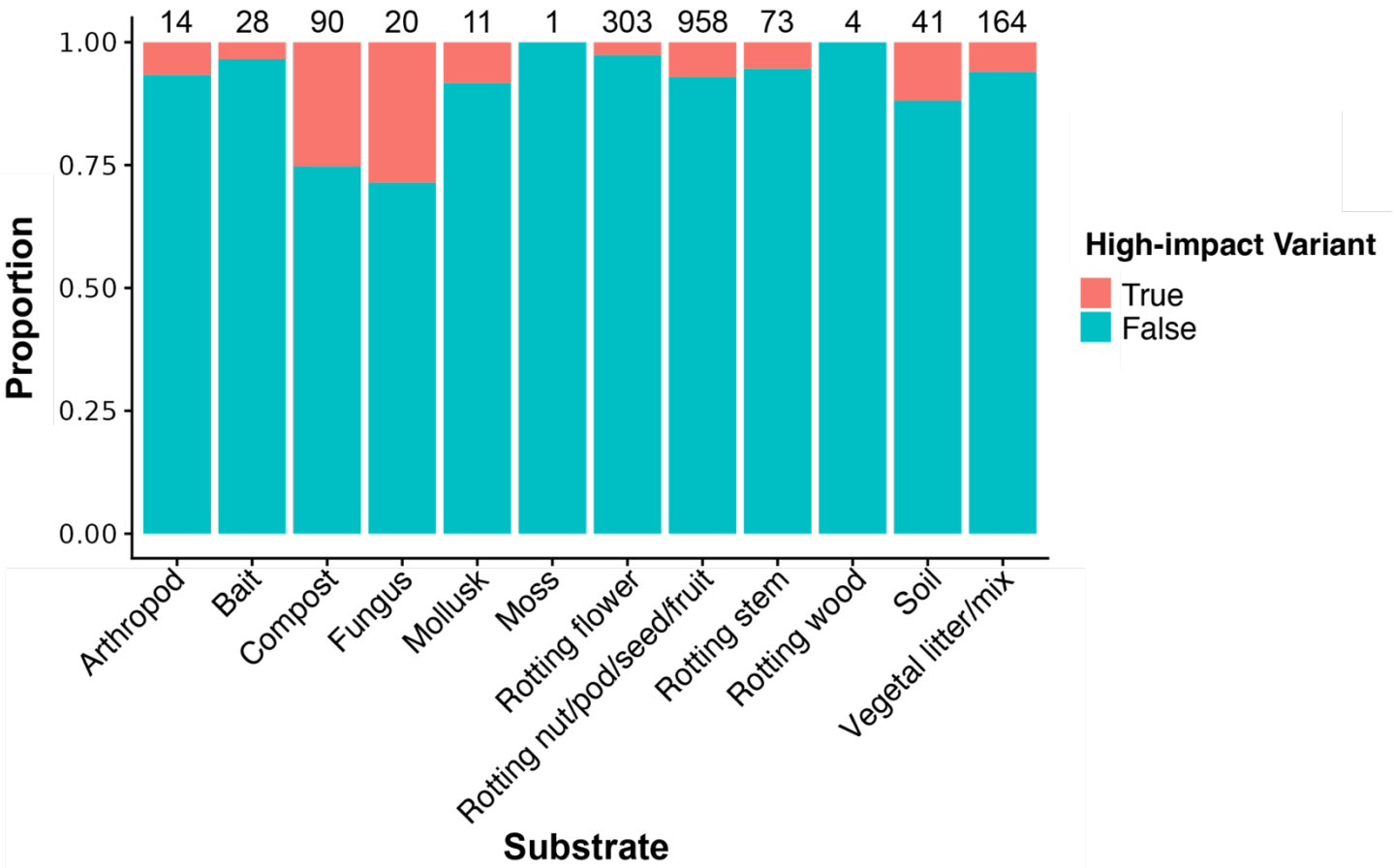

Supplemental Figure 15. The proportion of strains with high-impact resistant variants in beta-tubulin genes and the substrates where those strains were found
The proportion of strains (y-axis) found in a given substrate (x-axis) are displayed. Strains with a high-impact variant in a beta-tubulin gene are colored salmon. Strains with no variants in a beta-tubulin gene are colored teal. The total number of strains isolated from a given substrate is displayed above each column. Moss and rotting wood were not included in the substrate enrichment analysis due to the small sample size. No significant relationship between beta-tubulin gene variant status and substrate were identified (Fisher's Exact Test, p=1).